

Aus dem Max-Planck-Institut für Psychiatrie
Abteilung für Translationale Forschung in der Psychiatrie
Direktorin: Prof. Dr. Elisabeth Binder

**Enhanced Endocannabinoid Signaling Modulates Neuronal
Network Dynamics in the Hippocampus**

Dissertation
zum Erwerb des Doktorgrades
an der Medizinischen Fakultät der
Ludwig-Maximilians-Universität München

vorgelegt von

Jens Stepan

aus

Bremen

2018

**Mit Genehmigung der Medizinischen Fakultät
der Universität München**

Berichterstatterin:

Priv. Doz. Dr. med. Angelika Erhardt

Mitberichterstatter:

Prof. Dr. Nikolaos Koutsouleris

Priv. Doz. Dr. Johannes Levin

Mitbetreuung durch die promovierten Mitarbeiter:

Priv. Doz. Dr. rer. nat. Carsten Wotjak

Dr. rer. nat. Matthias Eder

Dekan:

Prof. Dr. med. dent. Reinhard Hickel

Tag der mündlichen Prüfung:

26.04.2018

Contents

Abbreviations	vi
List of Tables	viii
List of Figures	ix
Abstract	x
Zusammenfassung	xi
Eidesstattliche Versicherung	xii
Acknowledgments	xiii
1 Introduction	1
1.1 The endocannabinoid-system (ECS)	3
1.2 The hippocampus (HIP)	6
1.3 Foundations of voltage-sensitive-dyes	9
2 Aims of the thesis	12
3 Material and Methods	13
3.1 Animals	13
3.2 Preparation and staining of brain slices	14
3.3 Brain slice experiments	14
3.4 Voltage-sensitive dye imaging (VSDI)	15
3.5 Processing and quantification of VSDI data	16
3.6 Electrical stimulation techniques	17
3.7 Chemicals	18
3.8 Statistics	18
4 Results	19
4.1 Opposing effects of diazepam and AM404 on HTC-Waves	21
4.2 AM404 effects are mediated by D1R positive neurons	23
4.3 Hippocampal subregion specific drug effects	24

5 Discussion	26
6 Bibliography	31
7 Appendix	42
7.1 Chemicals	42

Abbreviations

2-AG	2-arachidonylglycerol, page 3
ACSF	artificial cerebrospinal fluid, page 18
AD	antidepressant, page 1
AEA	N-arachidonoyl-ethanolamine, page 3
AXDs	anxiety disorders, page 1
BDZ	benzodiazepines, page 2
BIM	bicuculline methiodide, page 14
CA	cornu ammonis, page 6
CB	cannabinoid, page 3
CB1R	cannabinoid 1 receptor, page 3
CB2R	cannabinoid 2 receptor, page 3
CBR	cannabinoid receptor, page 3
CCD	charged coupled device, page 15
D1R	dopamine 1 receptor, page 13
DG	dentate gyrus, page 6
DMSO	dimethyl sulfoxide, page 14
DSE	depolarization induced-suppression of excitation, page 5
DSI	depolarization induced-suppression of inhibition, page 5
EC	entorhinal cortex, page 6
eCB	endocannabinoids, page 3
eCB-LTD	endocannabinoid-mediated long-term depression, page 5
eCB-STD	endocannabinoid-mediated short-term depression, page 5
ECS	endocannabinoid-system, page 2
FAAH-1	fatty acid amide hydrolase-1, page 4
FDS	fast depolarization-mediated signal, page 17
GABA	gamma-aminobutyric acid, page 2
GCL	granule cell layer, page 8
GPCR	G-protein coupled receptor, page 3

HF	<u>hippocampal</u> <u>formation</u> , page 6
HIP	<u>hippocampus</u> , page 2
HPA	<u>hypothalamic-pituitary-adrenal</u> , page 29
HTC	<u>hippocampal trisynaptic circuit</u> , page 9
KO	<u>knockout</u> , page 13
LEC	<u>lateral entorhinal cortex</u> , page 7
LTP	<u>long-term potentiation</u> , page 28
MD	<u>major depression</u> , page 1
MEC	<u>medial entorhinal cortex</u> , page 7
MGL	<u>monoacylglycerol lipase</u> , page 4
ML	<u>molecular layer</u> , page 7
MPIP	<u>Max Planck Insitute of Psychiatry</u> , page 13
PARA	<u>parasubiculum</u> , page 6
PCL	<u>pyramidal cell layer</u> , page 8
PL	<u>polymorphic layer</u> , page 8
PP	<u>perforant pathway</u> , page 8
PRE	<u>presubiculum</u> , page 6
ROI	<u>region of interest</u> , page 16
SL	<u>stratum lucidum</u> , page 8
SLM	<u>stratum lacunosum-moleculare</u> , page 8
SO	<u>stratum oriens</u> , page 8
SR	<u>stratum radiatum</u> , page 8
SRPDs	<u>stress-related psychiatric disorders</u> , page 1
SSRIs	<u>selective serotonin reuptake inhibitors</u> , page 1
SUB	<u>subiculum</u> , page 6
TCAs	<u>tricyclic antidepressants</u> , page 1
TRPV1	<u>transient potential receptor of vanniloid 1</u> , page 4
USA	<u>United States of America</u> , page 14
VSDI	<u>voltage-sensitive-dye imaging</u> , page 10
WT	<u>wild-type</u> , page 13

List of Tables

7.1	Chemicals	42
-----	---------------------	----

List of Figures

1.1	Endocannabinoid-mediated short-term depression (eCB-STD)	5
1.2	Anatomy of the hippocampal formation	7
1.3	Physical mechanism of electrochromism	10
3.1	Deafferentations in hippocampal brain slices	15
3.2	Voltage-sensitive dye imaging setup	16
3.3	Quantification of VSDI signals	17
4.1	Experimental setup for recordings of polysynaptic activity flow through the HTC network	19
4.2	Anatomical position of ROIs and experimental protocol	20
4.3	Hippocampal activities in response to 5 Hz EC/DG-input	21
4.4	DMSO effect on HTC-Waves	22
4.5	Diazepam effect on HTC-Waves	22
4.6	AM404 effect on HTC-Waves	23
4.7	CB1Rs on D1R positive neurons mediate AM404 effects	24
4.8	CA3/CA1 activity ratios are drug specific	25

Enhanced Endocannabinoid Signaling Modulates Neuronal Network Dynamics in the Hippocampus

Abstract

The incidence of stress-related psychiatric disorders (SRPDs) such as major depression (MD), or anxiety disorders is constantly rising, while there is no effective and reliable pharmacotherapy. A breakthrough is not yet in sight and even worse, many pharmaceutical companies have stopped their drug development programs. This precarious situation affecting patients, therapists, and healthcare systems is caused by the demanding complexity of the mammalian brain, and its constant adaption to a variable environment. Current theories of SRPD aetiology involve multilevel dysregulation of molecular, cellular and neural circuit mechanisms. The endocannabinoid system (ECS) has a primary role in brain homeostasis, is altered in stress-related psychiatric disorders and appears as a new target for more efficient drugs. ECS modulator-induced behavioral changes are linked to hippocampal activity, but the alterations in millisecond-scale brain circuit dynamics that govern their cellular and molecular actions are largely unknown. Using a recently developed voltage-sensitive dye imaging assay in mouse brain slices it was tested, if the benzodiazepine diazepam and the endocannabinoid neurotransmission enhancer AM404 modulate neuronal activity propagation through the hippocampal trisynaptic circuit ("HTC": perforant path → dentate gyrus → area CA3 → CA1). While diazepam clearly reduced activity propagation through the HTC network ("HTC-Waves"), AM404 facilitated HTC-Waves in CA regions which was absent in mice lacking the expression of CB1 receptors on D1-receptor positive neurons. Collectively, these results show bidirectional drug effects on the HTC network, partly mediated via activity of a genetically defined neural population and point to the ECS as a therapeutic node for intervening with SRPDs.

Verstärkung der Endocannabinoid-vermittelten Neurotransmission moduliert die Netzwerkaktivität im Hippokampus

Zusammenfassung

Die Inzidenz von stress-assoziierten, psychischen Erkrankungen (SRPDs) wie Depressionen oder Angststörungen steigt stetig; eine effektive und zuverlässige medikamentöse Behandlung gibt es jedoch nicht. Ein Durchbruch ist nicht zu erwarten und schlimmer noch, viele pharmazeutische Unternehmen haben ihre entsprechenden Programme zur Medikamentenentwicklung gestoppt. Diese prekäre Situation mit Auswirkungen auf Patienten, Therapeuten und Gesundheitssysteme ist auf die Komplexität und ständige Anpassung des Säugergehirns zurückzuführen. Aktuelle Theorien zur Ätiologie von SRPDs beinhalten eine vielschichtige Dysregulation von molekularen Prozessen, zellulären Mechanismen und neuronalen Netzwerken. Das Endocannabinoidsystem (ECS) könnte ein neuer Ansatzpunkt für effektivere Medikamente sein, da es den Stoffwechsel des Gehirns maßgeblich beeinflusst und bei SRPDs in seiner Funktion beeinträchtigt ist. Durch Modulatoren des ECS hervorgerufene Verhaltensänderungen stehen in Zusammenhang mit der neuronalen Aktivität im Hippokampus (HIP). Dennoch ist über die zeitlich-räumliche Dynamik neuronaler Aktivität in Hirnschaltkreisen, welche durch Prozesse auf zellulärer und molekularer Ebene hervorgerufen wird, wenig bekannt. Daher wurde in dieser Arbeit mit Hilfe eines kürzlich entwickelten Bildgebungsverfahrens, das auf der Verwendung spannungssensitiver Farbstoffe basiert, untersucht, ob das Benzodiazepin Diazepam und der Verstärker der endocannabinoid-vermittelten Neurotransmission, AM404, den Aktivitätsfluss durch den trisynaptischen Schaltkreis des HIP ("HTC": perforant path → dentate gyrus → area CA3 → CA1) verändern. Diazepam reduziert den Aktivitätsfluss im HTC-Netzwerk ("HTC-Wellen"), während AM404 eine Verstärkung der HTC-Wellen hervorruft. Letzterer Effekt ist bei Mäusen ohne CB1 Rezeptoren auf D1 positiven Nervenzellen nicht nachweisbar. Zusammengefasst zeigen diese Ergebnisse diametrale Medikamenteneffekte im HTC-Netzwerk, die teilweise auf der Aktivität einer genetisch definierten Nervenzellpopulation basieren, und sie deuten auf eine wichtige Rolle des ECSs als therapeutisches Ziel zur Behandlung von SRPDs hin.

Eidesstattliche Versicherung

Stepan, Jens

Name, Vorname

Ich erkläre hiermit an Eides statt,

dass ich die vorliegende Dissertation mit dem Thema

Enhanced Endocannabinoid Signaling Modulates Neuronal Network Dynamics in the Hippocampus

selbständig verfasst, mich außer der angegebenen keiner weiteren Hilfsmittel bedient und alle Erkenntnisse, die aus dem Schrifttum ganz oder annähernd übernommen sind, als solche kenntlich gemacht und nach ihrer Herkunft unter Bezeichnung der Fundstelle einzeln nachgewiesen habe.

Ich erkläre des Weiteren, dass die hier vorgelegte Dissertation nicht in gleicher oder in ähnlicher Form bei einer anderen Stelle zur Erlangung eines akademischen Grades eingereicht wurde.

München, 01.03.2017

Ort, Datum

Unterschrift Doktorandin/Doktorand

Acknowledgments

The support of Carsten Wotjak and Matthias Eder was a substantial contribution to the success of this work. I would like to sincerely thank both of them.

A special thanks is also extended to Angelika Erhardt. She enabled me to carry out this dissertation at the faculty of medicine at the Ludwigs Maximilians University Munich.

Jens Stepan

Munich, March 2018

Chapter 1

Introduction

The causes of stress-related psychiatric disorders (SRPDs) including extremely debilitating diseases such as anxiety disorders (AXDs) and major depression (MD) remain largely unknown (Holsboer, 2008; Klengel and Binder, 2015). They significantly contribute to mortality and morbidity worldwide with a combined lifetime risk of around 30% (Kessler et al., 2005; Ressler and Mayberg, 2007; Steel et al., 2014). A cause or cure and objective diagnostic tests for SRPDs are missing because the underlying changes in brain function remain largely unknown (Cai et al., 2013). This fosters chronic illness, with significant emotional impact on patients, such that SRPDs are responsible for serious and constantly increasing constraints on healthcare systems (WHO, 2004). This lack of knowledge is mainly attributable to the multifactorial character of SRPDs, influenced by both genetic predisposition and environmental factors (Klengel and Binder, 2015). The term SRPDs is often used for various disease entities because multiple strands of evidence have identified similarities among these illnesses including: (i) stress as a common risk-factor, (ii) a high comorbidity, and, (iii) various shared molecular pathways and neurocircuits (Berton and Nestler, 2006; Ressler and Mayberg, 2007; Klengel and Binder, 2015).

Among different classes of psychotropic medication the most frequently used and first-line treatment option for most SRPDs are antidepressants (AD)s such as selective serotonin reuptake inhibitors (SSRIs) and tricyclic antidepressants (TCAs) (Ravindran and Stein, 2010). TCAs have been discovered by serendipity in the early 1950s, followed by SSRIs in the 1970s, and both elevate monoamine levels in the synaptic cleft (Wrobel, 2007). Despite steady advances in the understanding of monoamine signaling (Coleman et al., 2016), even the latest innovations reaching the market are "me-too" drugs, that is, they also inhibit monoamine reuptake from the synaptic cleft and need weeks of administration to become clinically effective (Berton and Nestler, 2006; Reardon, 2016). The recognition that ADs may be considered as a kind of "dirty drugs" that modulate by far more targets than monoamine levels and the discovery of fast symptom relief in SRPDs (Zanos et al., 2016), lead to considerable efforts on the discovery of more specific, faster acting drugs, that modulate non monoaminergic targets such as glutamatergic,

gamma-aminobutyric acid (GABA)ergic, neuroendocrine- and membrane-lipid derived transmitter systems (Rammes and Rupprecht, 2007; Micale et al., 2013; Carta et al., 2014; Zanos et al., 2016). Since all efforts have not yet succeeded in bringing any fundamentally new medications to the market and response rates of SRPDs to ADs are low, the pharmacological treatment fails in a considerable number of patients (Berton and Nestler, 2006; Lépine and Briley, 2011; Bandelow et al., 2014; Caddy et al., 2015; Zanos et al., 2016).

Because of the time lag before SSRIs and other medication become effective clinicians often prescribe benzodiazepines (BDZ) for acute symptom relief (Ravindran and Stein, 2010; Holsboer et al., 2012). In contrast to many other drugs they are effective immediately and their mode of action is well known. They bind to a specific subunit of the ionotropic GABA_A-receptor, the most abundant inhibitory receptor throughout the mammalian brain, resulting in an enhanced effect of the inhibitory neurotransmitter GABA (Holsboer et al., 2012). The GABAergic system is expressed in most brain regions (Watson et al., 2011). Thereby, BDZs have various effects including anxiolytic, amnesic, hypnotic, anticonvulsant, muscle-relaxant, and sedative actions (Ravindran and Stein, 2010; Hoffman and Mathew, 2008). The use of BDZs, though effective, is hampered by major side effects. From a clinical perspective, this includes over-sedation, psychomotor incoordination, and the risks of abuse and physiological dependence with long-term use. Especially the well documented cognitive impairment after BDZs administration is a serious problem because full cognitive performance seems to be superior for cognitive-behavioral therapy. Therefore, BDZs are recommended only for short-term use or in exceptional cases, e.g., suicidality and should be tapered once other medication becomes effective (Chouinard, 2004; Ravindran and Stein, 2010).

The endocannabinoid-system (ECS) is supposed to play a major role in SRPDs, thus, emerging as a target for the development of new drugs to treat these brain-based diseases more effectively (Hillard et al., 2012; Micale et al., 2013; Lutz et al., 2015). ECSs modulators were ascribed anxiolytic and antidepressant actions (Micale et al., 2013; Singewald et al., 2015; Pertwee, 2015; Rubino et al., 2015). A brain structure that is intimately linked to SRPDs with high expression levels of the ECS and therefore a potential target of ECS modulators is the hippocampus (HIP) (Krishnan and Nestler, 2008; Pertwee, 2015). But, the ECS represents a complex neurotransmitter-system and likewise ADs, pharmacological manipulation induces various molecular, cellular and structural changes (Kano, 2014; Pertwee, 2015). Recent research suggests, that it is difficult to integrate these manifold changes on the "microscale" for outcome prediction on the neuronal network level ("mesoscale") or even behavior ("macroscale"; Airan et al., 2007; Avrabos et al., 2013; Lewis and Lazar, 2013; Stepan et al., 2015b). Therefore, more circuit-centered approaches like voltage-imaging, calcium-imaging and optogenetics moved into the focus of neuroscience research and seem to be well suited to probe the functional aspects of "dirty-drugs" like ECS-modulators or ADs (Karayiorgou et al., 2012; Stepan et al., 2015b).

1.1 The endocannabinoid-system (ECS)

What is now known as the ECS is, like other neurotransmitter-systems, formed by distinct elements that enable signal transduction at chemical synapses and was started to be scientifically characterized in the 1960s (Bear and Paradiso, 2016; Mechoulam et al., 2014). These are: (1) at least two seven transmembrane domain-containing $G_{i/o}$ -protein coupled cannabinoid receptor (CBR)s, cannabinoid 1 receptor (CB1R) and cannabinoid 2 receptor (CB2R), that modulate diverse targets and appending signal transduction pathways (Matsuda et al., 1990; Munro et al., 1993), (2) several endogenous (hence endocannabinoids (eCB)) ligands of CBR, with the two best characterized and most abundant being N-arachidonoyl-ethanolamine (AEA) (anandamide) and 2-arachidonylglycerol (2-AG) (Devane et al., 1992; Mechoulam et al., 1995; Sugiura et al., 1995), (3) enzymes and processes responsible for the biosynthesis and removal or degradation of eCB (Di Marzo and De Petrocellis, 2012; Castillo et al., 2012; Pertwee, 2015; Cascio and Marini, 2015). The ECS modulates neurotransmission between multiple cell types in the brain, thereby regulating neuronal network activity and finally behavioral outputs. Because the ECS is also present in non neuronal tissue a variety of physiological processes have been identified that are modulated by eCB including immune response, cardiovascular function and metabolism (Marsicano and Lutz, 1999; Lutz et al., 2015; Krentz et al., 2016). Especially its role in the control of appetite, energy expenditure and aspects of glucose and lipid metabolism is worth mentioning, since the selective, inverse CB1R-agonist SR141716 Rimonabant is one of the few drugs targeting the ECS that has been approved for pharmacological support of weight reduction in 2006 (Krentz et al., 2016). But, already 2009 Rimonabant was withdrawn from the market due to psychiatric adverse events including anxiety, depression and suicidal ideation, supporting the ECSs diverse impact on physiological processes (Krentz et al., 2016). Although many researchers studied the components and function of the ECS and the topic attracted a great deal of attention in public because it is responsible for the effects of the cannabinoid (CB) delta-tetrahydrocannabinol (THC) which mediates the psychotropic activity of marijuana (*cannabis sativa*), the precise function of the ECS remains elusive (Gaoni and Mechoulam, 1971; Micale et al., 2013). The CB1R is perhaps the most common G-protein coupled receptor (GPCR) throughout the mammalian brain and is predominantly found at presynaptic terminals of central and peripheral neurons. It is highly expressed in cortical areas, amygdala, striatum, and cerebellum. CB1Rs were found in several neuronal subtypes at different expressions levels including glutamatergic, cholinergic, GABAergic, dopaminergic, noradrenergic, and serotonergic neurons, with highest levels in GABAergic neurons, but also in glia cells and microglia which are important for synthesis and degradation of eCB. Expression patterns also differ across subregions suggesting a complex mechanism to underlie the modulatory effects of eCB likely explaining their diverse effects on multiple physiological processes (Marsicano and Lutz, 1999; Haring et al., 2012; Micale et al., 2013; Pertwee, 2015). The CB2R was supposed to be mainly expressed outside of the nervous system, but recent research suggests its presence in glial cells and neurons of several brain regions such as amygdala, HIP and cerebral cortex (Hu and Mackie, 2015; Pertwee, 2015;

Stempel et al., 2016). In a recent study Stempel et al. (2016) describe a CB2R-mediated cell type-specific plasticity mechanism in the HIP that provides evidence for their neuronal expression and highlights their importance in neurotransmission (Stempel et al., 2016). A third CBR (CB3R) was also reported, but to date its role in regulating body function has not been definitively established (Micale et al., 2013).

Aside AEA and 2-AG, several other endogenous compounds that can activate or block cannabinoid receptors either orthosterically or allosterically were identified including noladin ether, virodhamine, dihomono- γ -linolenylethanolamide, sphingosine, docosate-traenoylethanolamide, N-arachidonoyldopamine, eicosapentaenoylethanolamide, docosahexaenoylethanolamide, N-oleoyldopamine and oleamide (Pertwee, 2015). Conversely, non-CBR-mediated pharmacological actions of eCB were reported. AEA and 2-AG bind to other GPCRs (GPR55, Muscarinic M1/M4, Adenosine A3, 5-HT1/5-HT2), ligand-gated ion channels (5-HT3, nicotinic, glycine, NMDA, GABA_A), ion-gated ion channels (T-type calcium Ca_v3, 2_{TM} potassium K_{ATP}, 6_{TM} potassium K_v), TRP channels (transient potential receptor of vanilloid 1 (TRPV1) (non-selective cation channel, to which vanilloids such as capsaicin bind), TRPM8) nuclear receptors α (PPAR- α) and γ (PPAR- γ) (Di Marzo and De Petrocellis, 2012; Pertwee, 2015). An important difference between the two most studied eCBs, 2-AG and AEA, are the metabolic pathways that underlie their biosynthesis and degradation (Di Marzo and De Petrocellis, 2012). Although contradicting results were reported (Hashimoto et al., 2013), both classical eCBs are usually produced on demand in postsynaptic sites, in response to elevation of intracellular Ca²⁺. AEA is synthesized from phosphatidylethanolamines on various biosynthetic pathways in a multistep process involving several, partly, yet not identified enzymes including N-acyl-phosphatidylethanolamine specific phospholipase D (NAPE-PLD), α,β -hydrolase-4 (ABHD4), glycerophosphodiesterase-1 (GDE1), an as-yet-unidentified phospholipase C (PLC) and other phosphatases. The most accepted pathway in the formation of 2-AG by hydrolysis of membrane phospholipids is catalyzed by the consecutive action of phospholipase C β (PLC β) and diacylglycerol lipase α (DGL α). AEA and 2-AG breakdown is catalyzed by intracellular enzymes, this is primarily monoacylglycerol lipase (MGL) and to a lesser extent α,β -hydrolase-6 (ABHD6), α,β -hydrolase-12 (ABHD12) for 2-AG and fatty acid amide hydrolase-1 (FAAH-1) for AEA. Furthermore, a hitherto not clearly identified membrane transporter for cellular uptake of eCBs has been reported, but its existence and putative mode of action is still a matter of debate (Glaser et al., 2003; Di Marzo and De Petrocellis, 2012; Fowler, 2013).

The basic mechanism by which eCB modulate synaptic function is through retrograde signaling. This mode of synaptic transmission is best characterized in the ECS where elevation of intracellular Ca²⁺ upon postsynaptic depolarization, activation of G_{q/11}-coupled and other receptors triggers de-novo synthesis of eCB (Figure 1.1). Subsequently, eCBs move retrogradely across the synapse by a unknown mechanism, bind presynaptic CB1Rs, and suppress neurotransmitter release by activation of A-type and inwardly rectifying K⁺ channels, and by inhibition of N- and P/Q-type Ca²⁺ currents (Alger and Kim, 2011; Castillo et al., 2012; Ohno-Shosaku and Kano, 2014; Kano, 2014; Pertwee, 2015). This

form of short-term synaptic plasticity is known as endocannabinoid-mediated short-term depression (eCB-STD) or more specifically depolarization induced-suppression of inhibition (DSI) and depolarization induced-suppression of excitation (DSE) at inhibitory and excitatory neurons, respectively (Kreitzer and Regehr, 2001; Ohno-Shosaku et al., 2001; Wilson and Nicoll, 2001). In several brain areas including the HIP, more physiological synaptic activity induces eCB-STD, mediated by postsynaptic AMPA receptors (Kano, 2014). A persistent reduction of transmitter release mediated by endocannabinoids is called endocannabinoid-mediated long-term depression (eCB-LTD) (Kano, 2014). 2-AG seems to be the principal eCB required for activity-dependent retrograde signaling which is supported by the observation that DGL α is mainly expressed in post-synaptic dendrites and somata, whereas CB1Rs and MGL are predominantly found in presynaptic terminals.

The biosynthesizing enzymes of AEA are located pre- and postsynaptically. FAAH-1 is predominantly found in post-synaptic locations and the enzymes are concentrated in intracellular membranes suggesting modulation of synaptic function by AEA in a non-retrograde, intracellular or autocrine manner (Castillo et al., 2012; Busquets Garcia et al., 2016). This can occur via postsynaptic TRPV1 channels and CB1Rs on or within (e. g. mitochondria) the postsynaptic cell (Castillo et al., 2012; Di Marzo and De Petrocellis, 2012; Busquets Garcia et al., 2016). Binding of AEA to TRPV1 channels (AEA is a full agonist at TRPV1 channels) received much attention because this interaction is involved in the induction of long-term depression in the HIP and nucleus accumbens supporting its hitherto questioned physiological relevance (Chávez et al., 2010; Di Marzo, 2010). Because biosynthesis and breakdown of AEA and 2-AG are different, it was suggested that they can act independently and simultaneously even if expressed at the same synapse. Different expression patterns of the ECS in distinct neuronal subpopulations, in different anatomical positions of a neuron, in specific pre-, post-, and extrasynaptic positions as well as extra- and intracellular membranes, and the finding that CBRs have more than one endogenous ligand allow diverse modulation of synaptic transmission and induction of synaptic plasticity on various time-scales (Di Marzo and De Petrocellis, 2012; Castillo et al., 2012; Ohno-Shosaku and Kano, 2014; Busquets Garcia et al., 2016). Moreover, the eCB itself

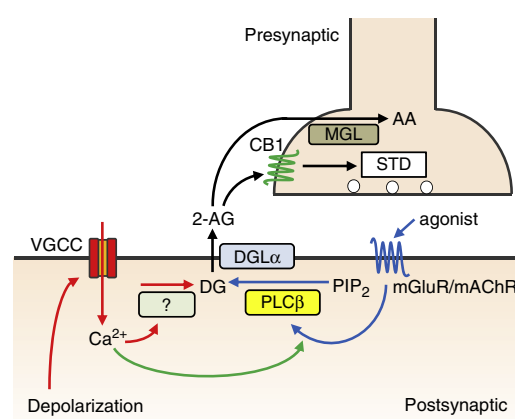


Fig. 1.1. Endocannabinoid-mediated short-term depression (eCB-STD). Diacylglycerol (DG) is synthesized by either a large Ca^{2+} elevation, caused by depolarization-induced activation of voltage-gated Ca^{2+} channels (VGCC) or NMDA-type glutamate-receptor (NMDAR, not illustrated), (red arrows), or strong activation of $G_{q/11}$ -coupled receptors such as mGluRs and mAChRs through PLC β (blue arrows). Subthreshold Ca^{2+} elevation and weak activation of $G_{q/11}$ -coupled receptors might exert synergistic effects on DG production (green arrow). DG is then converted to 2-AG by diacylglycerol lipase α (DGL α). 2-AG is subsequently released from the postsynaptic neuron, and activates presynaptic CB1Rs to suppress transmitter release. 2-AG is predominantly hydrolyzed to arachidonic acid (AA) by the presynaptic and intracellular enzyme monoacylglycerol lipase (MGL; adapted from Ohno-Shosaku and Kano, 2014).

Moreover, the eCB itself

undergoes plastic changes in response to diverse stimuli (Kano, 2014). To understand how the ECS regulates physical functions and for clinical use, a variety of substances have been developed for pharmacological intervention, although today no drug modulating the ECS is on the market (Micale et al., 2013). Among others this includes agonists/antagonists, inverse agonists, antibodies and ECS-enhancer (Micale et al., 2013; Singewald et al., 2015). Some of these substances exert their effects through direct interaction with CBRs like the selective, inverse CB1R-agonist SR141716 (Rimonabant; see this section above; Micale et al., 2013; Llorente-Berzal et al., 2015; Krentz et al., 2016). ECS-enhancers reduce the activity of the enzymes or transporters responsible for breakdown or removal of eCB thereby elevating extracellular eCB levels. A widely used substance is JZL 184, an irreversible inhibitor of MGL, which can elevate brain 2-AG-levels up to 8-fold (Micale et al., 2013). The bioactive N-acylamine AM404, a metabolite of the analgesic Acetaminophen (paracetamol; Hogestatt et al., 2005) is another prototypical eCB transport inhibitor with fear-alleviating/anxiolytic effects in several animal models and was used in the present study (see also Results (4.2) and Discussion (5); Beltramo et al., 1997; Zygmunt et al., 2000; Hogestatt et al., 2005; Micale et al., 2013). Like all other ECS-enhancers AM404 has the disadvantage, that its exact mode of action is not fully understood, likely due to the complexity of the ECS itself, its polypharmacological profile and potential interaction with other neurotransmitter systems (Micale et al., 2013; Pertwee, 2015; Singewald et al., 2015).

1.2 The hippocampus (HIP)

Because the HIP has anatomical features that have been a fertile ground for circuit-centered approaches and is a focus of psychiatric and eCB research, experiments were conducted in this limbic brain region (Marsicano and Lutz, 1999; Airan et al., 2007; Ressler and Mayberg, 2007; Stepan et al., 2012). Moreover, recent research points to the HIP as a potential target of eCB-modulators for pharmacological augmentation of psychotherapies (e. g. exposure-based therapies; see also Discussion (5)).

The HIP is a part of the hippocampal formation (HF), which is formed by six cytoarchitecturally distinct subregions including the dentate gyrus (DG), the ammon's horn (cornu ammonis (CA), with its subregions CA3, CA2 and CA1), the subiculum (SUB), the presubiculum (PRE), the parasubiculum (PARA), and the entorhinal cortex (EC) (Figure 1.2; Amaral and Witter, 1989).

The mouse HIP (here: DG and CA-subregions), is a long, curved structure lying in the temporal lobe of each hemisphere. It has a transverse axis ranging from the DG to CA-subregions (running in parallel to the cell layer) and a longitudinal, dorsoventral or septotemporal axis running from the septal nuclei rostrally to the temporal cortex ventrocaudally (Figure 1.2; Amaral and Witter, 1989; Amaral, 1993; Andersen et al., 2006). Multilevel analyses (genetic, molecular, behavior, functional and circuit) suggest a functional segmentation of the HIP along its rostral/caudal axis with roughly

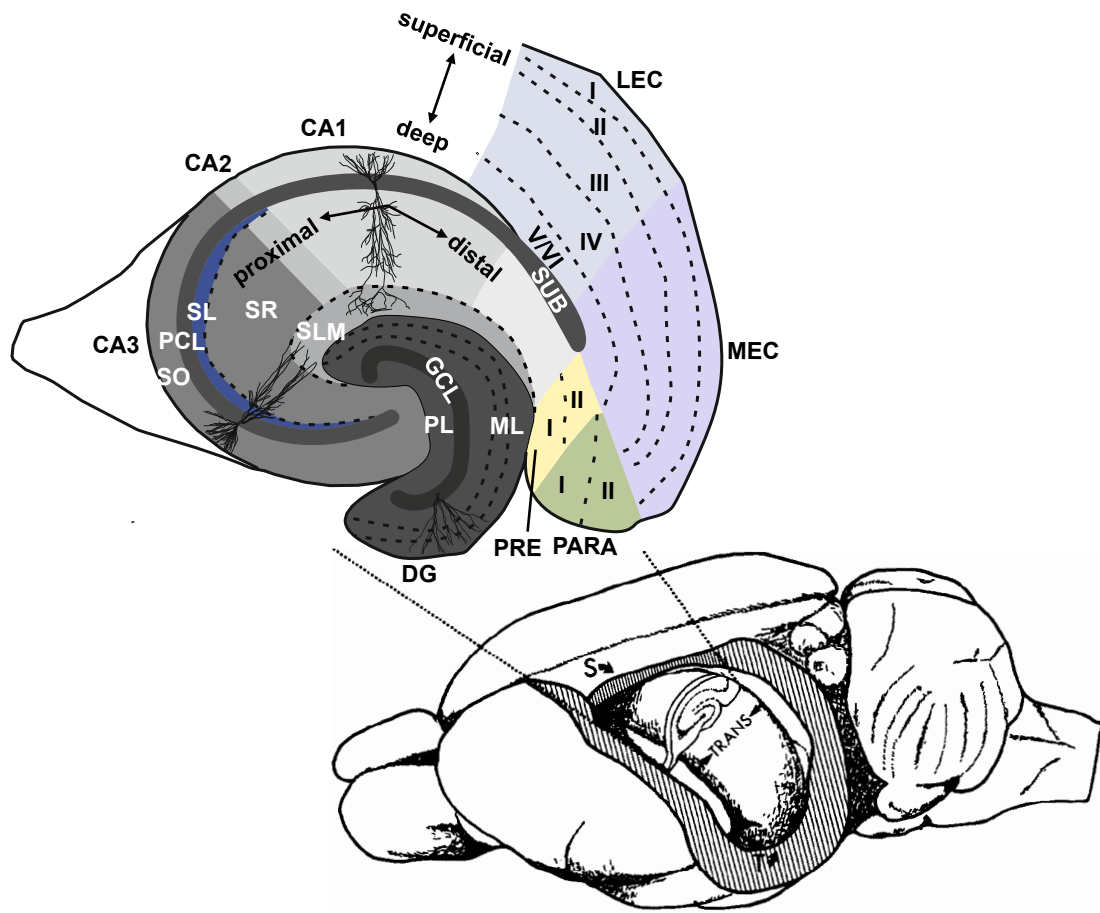


Fig. 1.2. Anatomy of the hippocampal formation. Expansion of the c-shaped HIP from the septal nuclei (S) to the temporal cortex (T) in the rodent brain (adapted from Amaral and Witter, 1989). The outtake illustrates a transverse section (TRANS) through the HIP (adapted from Stepan, 2015). Abbreviations: CA, cornu ammonis; GCL, granule cell layer; DG, dentate gyrus; LEC, lateral entorhinal cortex; MEC, medial entorhinal cortex; ML, molecular layer; PARA, parasubiculum; PCL, pyramidal cell layer; PL, polymorphic layer; PRE, presubiculum; SL, stratum lucidum; SLM, stratum lacunosum moleculare; SO, stratum oriens; SR, stratum radiatum; SUB, subiculum.

three subdivisions: dorsal/rostral (septal pole), intermediate, and ventral/caudal (temporal pole). The dorsal part is typically associated with cognitive functions like learning and memory or spatial navigation, whereas the ventral part is supposed to process information associated with stress, emotion and affect (Fanselow and Dong, 2010; Strange et al., 2014). More recently, a model that incorporates functional longitudinal-axis gradients, superimposed on discrete functional domains, provides a potential framework to explain the multiple functions ascribed to the HIP more precisely (Strange et al., 2014). In the EC, six sublayers are usually distinguished. Five of them are dominated by cell bodies, the most superficial one is called molecular layer (ML) and predominantly contains axons. Although this building plan is similar to the neocortex, the most prominent excitatory projection cells in the EC are stellate cells and pyramidal cells located in layers II and III. Distinct anatomical features and connectivity patterns as well as functional differences divide the EC into a medial part (medial entorhinal cortex (MEC)) and a lateral part (lateral entorhinal cortex (LEC)); Figure 1.2; Hafting et al., 2005; Andersen et al., 2006;

Patton and McNaughton, 1995; Watson et al., 2011; Stepan, 2015).

A prominent and recognizable feature of the DG is a "U"-shaped appearance in ventral parts, and a more "V"-shaped appearance in dorsal parts. Approximately one third of the DGs longitudinal extent is located between areas CA1 and CA3 and is called suprapyramidal or inner blade. Next follows the middle third, located at the kink of the "V" or "U", which is called the crest. The main input region of the HIP is completed by the last third, inferior to area CA3, which is called infrapyramidal or outer blade (Figure 1.2; Amaral et al., 2007; Claiborne et al., 1986; Patton and McNaughton, 1995; Witter, 2007; Stepan, 2015). The DG is composed of three layers which are usually divided into a deep layer adjacent to CA3 (hilus or polymorphic layer (PL)), a principal cell layer (granule cell layer (GCL)) with characteristic, densely packed granule cells, and a superficial ML. The GCL and ML are sometimes summarized as fascia dentata. The ML contains the perforant pathway (PP), an important axon bundle that conveys information to all subregions of the HIP. More specifically, it is formed by axons from EC layer II/III cells, which provide excitatory synaptic input on apical dendrites of DG granule cells (Figures 1.2, 4.1; Amaral et al., 2007; Patton and McNaughton, 1995; Claiborne et al., 1986; Watson et al., 2011; Witter, 2007; Stepan, 2015).

The CA is usually described as having three layers: A deep layer called stratum oriens (SO), characterized by the presence of the principal cells basal dendrites. A middle and most prominent layer, the pyramidal cell layer (PCL) or principle cell layer and a ML. The ML is divided into distinct sublayers that differ across CA subregions: (1) stratum lucidum (SL), containing proximal apical dendrites of pyramidal cells and is only present in areas CA2 and CA3; (2) stratum radiatum (SR), containing the distal apical dendrites of pyramidal neurons; (3) stratum lacunosum-moleculare (SLM) adjacent to the hippocampal fissure, comprising the pyramidal neurons apical tufts of the apical dendrites (Figure 1.2; Andersen et al., 2006; Kohara et al., 2014; van Strien et al., 2009; Stepan, 2015). Primarily neurons in deep layers IV and V of the EC receive information coming back from hippocampal output regions area CA1 and the subiculum. EC layer IV and V neurons subsequently project to superficial layers or high-order association cortices. EC layer II neurons also send axons via the PP directly to areas CA3 and CA2. Another input to the HIP emerges from EC layer III neurons projecting via the temporoammonic pathway (part of the PP) exclusively to the CA1 subfield and the subiculum. This circuitry suggests the EC to be the major hub between the HIP and other cortical regions (Figure 1.2, Witter et al., 2000; van Strien et al., 2009; Kohara et al., 2014; Stepan et al., 2015a).

In contrast to the reciprocal connectivity of most other cortical structures the anatomical features described above facilitate a unidirectional passage of information through the entorhinal-hippocampal loop via several parallel pathways. Before entering the HIP, polymodal sensory information is funneled through a hierarchically organized neocortical network and is subsequently fed into the EC, mainly to superficial layers II and III (Andersen et al., 2006; Teyler and Rudy, 2007; Stepan et al., 2015a; Backus et al.,

2016). Subsequently activated DG granule cells give rise to mossy fibers, the most prominent non-commissural/ associational excitatory innervation of CA3 pyramidal neurons. These cells in turn synapse via the glutamatergic Schaffer collaterals onto ipsilateral CA1 pyramidal neurons, thereby completing a highly topologically arranged loop of information flow, the hippocampal trisynaptic circuit (HTC) (Amaral and Witter, 1989; Kohara et al., 2014; Stepan et al., 2015a). Its prominent anatomical appearance and well-established role in various cognitive processes argues for the HTC as the main route of information flow through the HIP (Nicoll and Schmitz, 2005; Nakashiba et al., 2008; Neves et al., 2008; Daumas et al., 2009; Stepan et al., 2015a). Additionally, there is a previously unknown trisynaptic circuit. A subpopulation of DG granule cells target CA2 pyramidal neurons, which synapse on distinct CA1 counterparts. But, its function and mode of operation have yet to be clarified (Kohara et al., 2014; Stepan et al., 2015a). Beside the connectivity pattern described above, different subregions of the HIP are connected with subcortical structures including the amygdala, the hypothalamus, the medial septum, the raphe nucleus, and the locus coeruleus. Furthermore, the HIP has a substantial commissural input from the contralateral HIP and an ipsilateral associational loop (Nicoll and Schmitz, 2005; Andersen et al., 2006; Stepan et al., 2015a). Complicating the picture, the HIP also includes associational loops and partly complex interneuronal circuits which mediate feed-forward and/or feedback inhibition of principal neurons and disinhibition processes (Klausberger and Somogyi, 2008; Stepan et al., 2015a).

The gross anatomy of the HF and associated structures has important functional implications. Out of several parallel pathways, the trisynaptic circuit (EC layer II (PP) → DG → CA3 → CA1 output subfield), with its prominent appearance and principally unidirectional connectivity, is ideally suited to monitor polysynaptic activity flow within the mammalian central nervous system.

1.3 Foundations of voltage-sensitive-dyes

Significant advances in neuroscience research have traditionally been intimately linked to progress in methodological approaches to probe the complex function of the nervous systems in various species including humans (Neher and Sakmann, 1976; Klar and Hell, 1999; Zemelman et al., 2002). For functional analysis of the nervous system modern neuroscience offers various excellent techniques ranging from single-cell and local field potential recording to more indirect analysis of whole brain activity using functional magnetic resonance tomography (Neher and Sakmann, 1976; Andersen et al., 2006; deCharms, 2008; Stepan et al., 2015a). But, to study assemblies of neurons during information processing, these approaches are limited either by their spatial scale, because recordings from individual or a few neurons ("microscale") typically provide little information about the associated network, or by the facts that (1) non-invasive imaging methods ("macroscale") measure a surrogate signal whose spatial and temporal resolution is subject to both physical and biological constraints, and (2) widely used analysis software produce a high rate of false-positive results (Logothetis, 2008; Lewis and Lazar, 2013;

Stepan et al., 2015a; Eklund et al., 2016). To provide a better understanding of brain function, circuit-centered approaches which operate at the interface of the aforementioned methods are highly recommended (Karayiorgou et al., 2012; Lewis and Lazar, 2013; Stepan et al., 2015a). To directly study how neurons communicate across multiple synapses in large/mesoscale networks in real time, high-speed optical techniques like voltage-sensitive-dye imaging (VSDI) seem to be prerequisite to cover the methodologically demanding "mesoscale" of neuroscience research (Iijima et al., 1996; Airan et al., 2007; Refojo et al., 2011; Stepan et al., 2012; Avrabos et al., 2013; Stepan et al., 2015a; Stepan et al., 2015b).

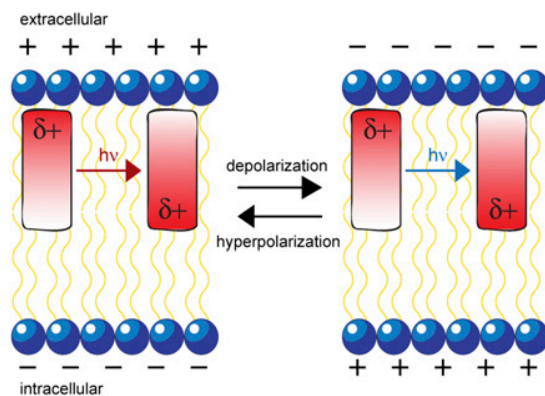


Fig. 1.3. Physical mechanism of electrochromism. Absorption of a photon significantly alters the charge distribution of the chromophore (strong induced dipole, excited state). Membrane potential changes (neuronal activity) influence the relative energy of the ground and excited states of the chromophore (hyperpolarization= stabilized, depolarization= the charge shift inverted state is destabilized), resulting in spectral shifts in the emission of the dye (adapted from Miller et al., 2012).

VSDI employs organic membrane-bound molecules. Their optical properties are often mediated by fluorescence or absorption, and various dye-specific molecular mechanisms that account for a (membrane) potential-dependent change of their optical properties have been described so far. These dyes in combination with advanced optics allow the analysis of neuronal activity on a millisecond scale, with micrometer-range spatial resolution and a scope spanning the entire brain circuits under investigation (Tominaga et al., 2000; Grinvald and Hildesheim, 2004; Airan et al., 2007; Carlson and Coulter, 2008; Chemla and Chavane, 2010; Stepan et al., 2012; Stepan et al., 2015b). Peterka

et al. (2011) emphasize that voltage-imaging might be the most appropriate technique for a complete description of the activity of neurons or of their subcellular compartments (Peterka et al., 2011). But, significant technical challenges associated with the biophysical constraints of the measurements themselves, might account for the more frequent use of alternative methods (e.g. calcium-imaging; Peterka et al., 2011). Biophysical mechanisms leading to voltage sensitivity in plasma membrane measurements include among others, repartitioning, reorientation, electrochromism or fluorescence resonance energy transfer (FRET) (Baker et al., 2005; Peterka et al., 2011; Miller et al., 2012). The dye used here, Di-4-ANEPPS, is a fast fluorescent styryl- dye that stably inserts into cytoplasmic membranes and is thought to sense changes in the surrounding electrical field via electrochromism. This is enabled by the core of Di-4-ANEPPS, a chromophore with large differences in its dipole moment that directly interacts with light (Fluhler et al., 1985; Peterka et al., 2011). Upon absorption of light the chromophore changes its electronic structure and moves from its ground state to its low-lying electronically excited state accompanied by a large internal charge transfer and large induced dipoles (Figure 1.3). These states are differentially stabilized by depolarizing and hyperpolarizing membrane

potentials, which changes the energy levels of the chromophore resulting in small spectral shifts in the emission of the dye (Canepari and Zecevic, 2010; Peterka et al., 2011; Miller et al., 2012). Di-4-ANEPPS's emission spectrum is shifted to longer (excited state molecular dipole is stabilized = hyperpolarization) or shorter (the charge shift inverted state is destabilized = depolarization) wavelengths (Figures 3.2 B; 1.3; Peterka et al., 2011; Miller et al., 2012; Stepan, 2015). This mechanism allows to differentiate between excited and/or unexcited tissue and to calculate the fractional change of fluorescence ($\Delta F/F$) for each pixel thus, reflecting a direct measurement of neuronal population activity (Canepari and Zecevic, 2010; Loew, 1992; Miller et al., 2012; Tominaga et al., 2000; Stepan, 2015). Because the electric field and the energy levels of the fluorophore directly interact, the kinetics of voltage sensing occur on a timescale commensurate with absorption and emission, resulting in ultrafast spectral emission shifts (fs to ps), many orders of magnitude faster than required to resolve action potentials (ms) in neurons (Miller et al., 2012; Stepan, 2015). Importantly, the magnitude of the wavelength shift is linearly related to the size of the change in potential resulting in a direct, fast, and linear measure of the change in membrane potential. Values for changes of ΔF in neuronal tissue stained with Di-4-ANEPPS typically range around 10% per 100 mV (Fluhler et al., 1985; Baker et al., 2005; Stepan, 2015).

Chapter 2

Aims of the thesis

Comprehensive research in various species, including humans, has shown that the hippocampus (HIP) plays a central role in stress-related psychiatric disorders (SRPDs) and provided substantial evidence that disease symptoms partly result from malfunction of information processing within the hippocampal network (Castrén, 2005; Ressler and Mayberg, 2007; Singewald et al., 2015; Pertwee, 2015). Furthermore, the endocannabinoid system (ECS), which is highly expressed in the HIP, seems to be dysregulated in SRPDs, providing a potential target for pharmacological intervention (Micale et al., 2013). Whereas classical electrophysiology shed light on the function of single cells and small neuronal populations these methods however, provide a limited and possibly distorted picture of how large/meso-scale neuronal networks respond to pharmacological intervention in real time (Lewis and Lazar, 2013). In recent years methods like optogenetics, calcium-imaging, voltage-sensitive-dye imaging (VSDI) or their combination ("all optical") provide more circuit-centered approaches for the analysis of disease related neuronal network activity (Karayiorgou et al., 2012; Emiliani et al., 2015). Within this framework, the present dissertation intended to address two major questions:

1. First, does a commonly used drug to treat the symptoms of SRPDs (diazepam) and an endocannabinoid system-enhancer (AM404), modulate neuronal network dynamics in the HIP?
2. Second, which receptor(s) mediate(s) putative effect(s) of AM404 on neuronal network dynamics in the HIP?

To address these questions VSDI was applied to mouse brain slices. VSDI allows the analysis of neuronal activity on a millisecond time-scale, with a micrometer-range spatial resolution and, most notably, a scope spanning the entire HIP (Airan et al., 2007; Peterka et al., 2011; Stepan et al., 2012; Stepan et al., 2015a).

Chapter 3

Material and Methods

3.1 Animals

Male C57BL/6N mice were purchased from the MPI of Biochemistry (Martinsried, Germany) at an age of 8-12 weeks. Male conditional dopamine 1 receptor (D1R)-CB1R^{-/-} mice (mice lacking CB1Rs on D1R-expressing neurons in the forebrain, D1R-CB1R-knockout (KO) and their respective wild-type (WT) littermate controls (D1R-CB1R^{+/+}, D1R-CB1R-WT) were provided by Carsten T. Wotjak, and tested at an age of 12-16 weeks. In brief, conditional D1R-CB1R-KO mice were generated by crossing a mouse line in which the CB1 coding region is flanked by two loxP sites (CB1-floxed mice, CB1^{f/f}), with a transgenic mouse line where Cre recombinase is expressed under the control of the regulatory sequences of a cell type specific promotor, here, of the dopamine receptor D1 (D1-Cre; Marsicano et al., 2003; Monory et al., 2007). In these mice the CB1 receptor is deleted in all D1 receptor expressing neurons of the forebrain but maintains its expression in the rest of the brain. All animals were housed one to five per standard cage (25 x 19 cm) at the animal facility of the Max Planck Institute of Psychiatry (MPIP) in Munich. The animals received food and water *ad libitum* and temperature and humidity were maintained constant (22 °C ± 1 °C; relative humidity 55% ± 10%) with a 12 h light/dark cycle (lights on from 7:00 A.M. to 7:00 P.M.). All experimental procedures were approved by the Committee of Animal Health and Care of the local governmental body and were performed in strict compliance with the guidelines for the care and use of laboratory animals set by the European Community.

3.2 Preparation and staining of brain slices

Mice were anesthetized with isoflurane (see Appendix 7.1) and decapitated at the level of the cervical spinal cord using an animal guillotine. All following steps were done in ice-cold homogenized and partially frozen sucrose-based saline (Bischofberger et al., 2006). The saline (pH 7.4) was saturated with carbogen gas (95% O₂/5% CO₂) and consisted of (in mM): 87 NaCl, 2.5 KCl, 25 NaHCO₃, 1.25 NaH₂PO₄, 0.5 CaCl₂, 7 MgCl₂, 25 glucose, and 75 sucrose. After decapitation, the head was transferred into a petri dish and the brain was rapidly removed from the cranial cavity. Next, the brain was separated into its hemispheres. The right hemisphere was prepared for the slicing procedure by a special transversal cut, which is sometimes called "magic cut", to maintain the intrahippocampal axonal projections as good as possible (Bischofberger et al., 2006). Next, the brain was glued with the "magic cut" side on a cooled tissue block with a tissue adhesive made from enbucrilate (Histoacryl[®]; Aesculap AG; Tuttlingen; Germany). Then the tissue block was immediately placed into the cutting chamber of a vibratome (HM650V, Freq.: 66, Ampl.: 0.9, V=8; Thermo Scientific; Waltham; United States of America (USA)). Subsequently, 350 μ m-thick horizontal slices containing the HIP were cut with a cleaned (acetone, ethanol) razor blade (Dreaming; Goldhand mbH; Düsseldorf; Germany) and transferred into a maintenance chamber. According to Bischofberger et al. (2006), the angle between blade and horizontal plane was set at $\sim 17^\circ$. After preparation, slices were incubated in carbogenated sucrose-based saline for at least 30 min at 34 °C. Subsequent staining of brain slices with the voltage-sensitive dye Di-4-ANEPPS (see 7.1; Tominaga et al., 2000; Airan et al., 2007; Refojo et al., 2011; Stepan et al., 2012; von Wolff et al., 2011, dissolved in dimethyl sulfoxide (DMSO) to a 20.8 mM stock solution) was carried out at room temperature (23 – 25 °C). For staining, slices were kept for 15 min in carbogenated physiological saline containing Di-4-ANEPPS (7.5 g/ml; <0.1% DMSO; Refojo et al., 2011; von Wolff et al., 2011). The physiological saline (pH 7.4) consisted of (in mM): 125 NaCl, 2.5 KCl, 25 NaHCO₃, 1.25 NaH₂PO₄, 2 CaCl₂, 1 MgCl₂, and 25 glucose. Afterwards, slices were transferred back to the maintenance chamber and stored at room temperature for a minimum of 30 min in Di-4-ANEPPS-free, but bicuculline methiodide (BIM)-containing (0.6 μ M, for rationale see (Stepan et al., 2012)) carbogenated physiological saline.

3.3 Brain slice experiments

VSDI was conducted at room temperature on a vibration-cushioned table (TMC; Peabody; USA), equipped with a Faraday cage (TMC; Peabody; USA) to minimize extraneous electrical noise. In a submerged-type recording chamber, slices were fixed with a custom made platinum frame/nylon string harp ("grid") and continuously superfused with BIM (0.6 μ M), containing carbogenated physiological saline (4-5 ml/min flow rate). The circulation was established by using a combination of a gravity system (for influx) and a peristaltic pump (Ismatec; Glattburg; Germany; for outflow). Thus, vibrations at the

surface of the superfusion medium were reduced. These settings avoid motion artifacts which is paramount for optical recordings. Figure (3.1A) depicts one representative slice that was cut at a distance between 2.3 and 3.0 mm (± 0.1 mm) from the ventral base of the brain. Previous research revealed that hippocampal trisynaptic circuit (HTC)-Waves can be most reliably evoked in these particular slices (Stepan et al., 2012; Stepan et al., 2015b). According to the "ventral/dorsal HIP hypothesis" (see 1.2; Maggio and Segal, 2007; Fanselow and Dong, 2010), experiments were conducted in the dorsal HIP or in the intermediate zone. EC/DG-input was evoked by patterned electrical stim-

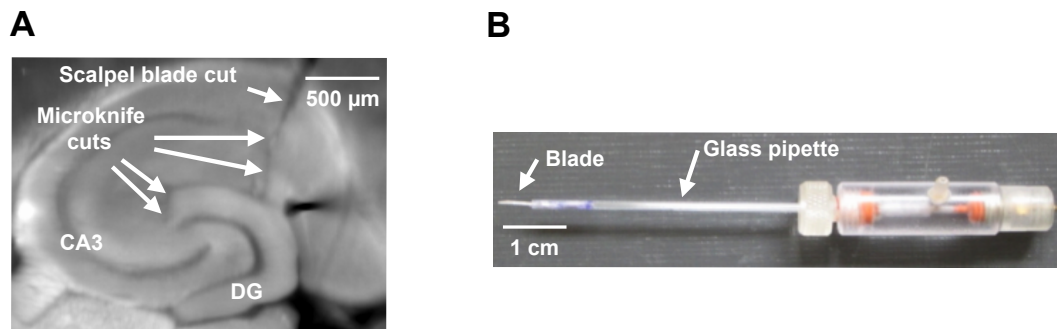


Fig. 3.1. Deafferentiations in hippocampal brain slices. (A) Illustration of deafferentiations performed with a scalpel blade and the microknife in hippocampal brain slices. (B) Custom made microknife used for cutting direct cortical inputs to areas CA3 and CA1 (A, modified from Stepan et al., 2012, B, adapted from Stepan, 2015).

ulation of the PP, which also contains EC layer II projections which travel in the ML of the DG and directly innervate distal apical dendrites of CA2 and CA3 pyramidal neurons (Kohara et al., 2014). After fixation of the slice, but before placing stimulation or recording electrodes, these fibers were cut at the tip of the suprapyramidal blade, the point where they exit the DG (Andersen et al., 2006, Figure 3.1A). Temporoammonic (EC layer III) projections that directly innervate the most apical dendrites of CA1 pyramidal neurons were likewise functionally inactivated by a cut, ranging from the hippocampal fissure to the cortical surface (Figure 3.1A, Andersen et al., 2006). The deafferentiations were accomplished by a tapered scalpel blade and a custom-made "microknife" (approximately 100 μ m blade length; Figure 3.1A,B; Stepan et al., 2012).

3.4 Voltage-sensitive dye imaging (VSDI)

VSDI and data analysis were performed using the MiCAM02 hard- and software package (BrainVision; SciMedia Ltd.; Costa Mesa; USA). The tandem-lens fluorescence microscope was equipped with the MiCAM02-HR camera (charged coupled device (CCD) camera) and a 2x and 1x lens at the objective and condensing side, respectively (Figure 3.2A).

By a halogen light source (MHAB; 150W; Moritex Corp.; Tokyo; Japan), an excitation filter (530 nm pass) and a dichroic mirror (520 ~ 560 nm reflect (>90%), 600 nm (>85%)

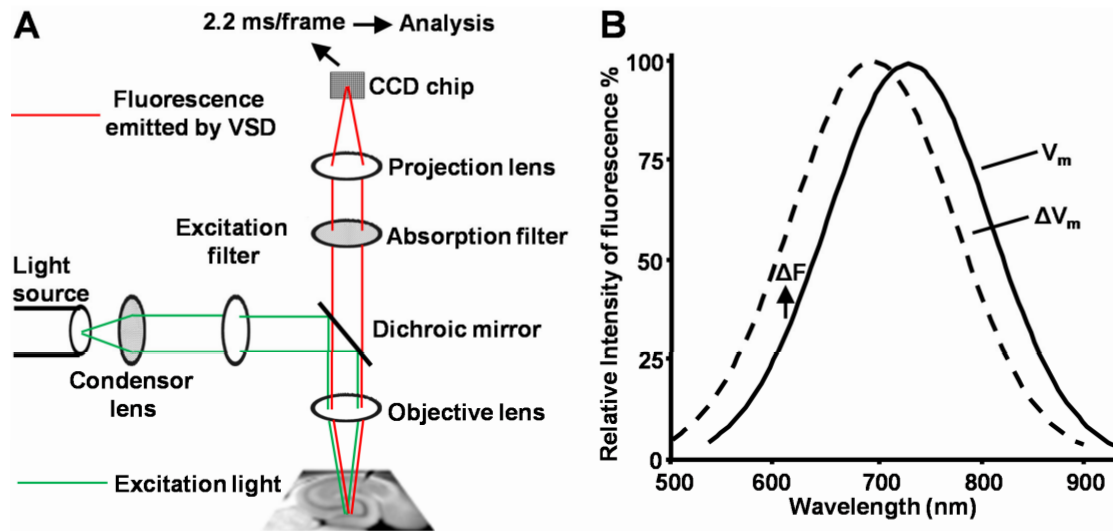


Fig. 3.2. Voltage-sensitive dye imaging setup. (A) Components used for imaging of neuronal activities via fluorescence emitted from voltage-sensitive dyes, recorded with a CCD camera. (B) Electrochromic voltage-sensitive dyes are believed to sense a change in the surrounding electric field via electrochromism or the molecular Stark effect. Upon depolarization, the emission spectrum of Di-4-ANEPPS shifts to shorter wavelengths with a concomitant decrease of the area under the curve (ΔF) of integrated wavelengths > 590 nm. (A, adapted from Stepan, 2015), B, modified from Canepari and Zecevic, 2010, p.16). Abbreviations: ΔF , change in fluorescence; V_m , membrane voltage; VSD, voltage-sensitive dye.

pass), the light was reflected towards the objective lens to illuminate the brain slice, stained with Di-4-ANEPPS. Subsequently, the fluorophore Di-4-ANEPPS emits photons (fluorescence) that were collected and projected onto the CCD sensor through an emission filter (> 590 nm; Figure 3.2A; Tominaga et al., 2000). Unless noted otherwise, standard settings of the MiCAM02-HR camera system were as follows: 88×60 pixels frame size, $36.4 \times 40.0 \mu\text{m}$ pixel size, and 2.2 ms sampling time.

3.5 Processing and quantification of VSDI data

From recorded VSDI signals, $\% \Delta F/F$ for wavelengths > 590 nm was calculated (Figure 3.2B). For all quantifications, $\% \Delta F/F$ values were spatially and temporally smoothed, using a $3 \times 3 \times 3$ average filter. VSDI signals presented in images were smoothed with a $5 \times 5 \times 3$ average filter. To attenuate slow signal components produced from bleaching of the voltage-sensitive dye (Carlson and Coulter, 2008) and a slight summation of 5 Hz neuronal responses, a weak high-pass filter of the MiCAM02 software was applied ($\tau = 220$ ms) to the imaging data afterwards. Pixelation of images was reduced by the interpolation function of the MiCAM02 software. For analysis of neuronal population activity in hippocampal subregions, three standardized region of interest (ROI) were manually set according to anatomical landmarks. The circular CA3-ROI ($r = 4$ pixels) was placed into the CA3 region close to the DG, but not overlapping with it. The circular CA1-ROI ($r = 4$ pixels) was positioned into the CA1 subfield at a distance of $\sim 200 \mu\text{m}$ from the

visually identified distal end of the stratum lucidum. The CA3-, and CA1-ROI spanned the stratum oriens, stratum pyramidale, and stratum lucidum/radiatum (Figure 4.2A).

The polygon DG-ROI (composed of ~ 450 pixels) enclosed the outer two layers of the DG (without the hilus) and was created by the polygon-drawing function of the Mi-CAM02 software (Figure 4.2A). The average of smoothed $\% \Delta F/F$ values within a particular ROI served as a measure of neuronal population activity. For further analysis in BrainVision, the peak amplitude of the fast depolarization-mediated signal (FDS) was corrected (Figure 3.3), to avoid that background fluorescence (noise) biased FDS values during pharmacological experiments. As a final measure of neuronal activities the last FDS in area CA3 and CA1, and the the first FDS in the DG were used (Figure 4.2B). From all data presented in absolute values (only for illustration of results) the peak amplitude was calculated in Excel (Version 2003; Microsoft; Redmond; USA) without applying the correction procedure.

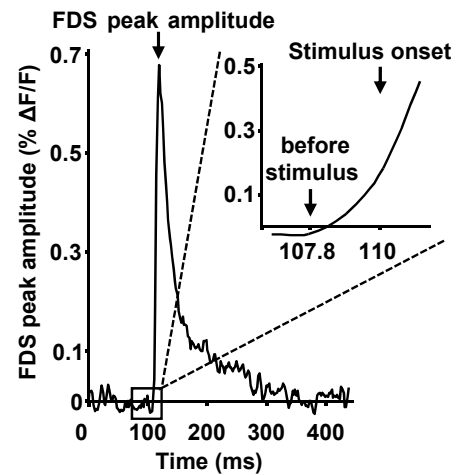


Fig. 3.3. Quantification of VSDI signals. To quantify FDSs, the value ($\% \Delta F/F$) before stimulus onset (107.8 ms) was subtracted from the value at FDS peak amplitude (adapted from Stepan, 2015).

3.6 Electrical stimulation techniques

In all experiments, neuronal activity was evoked by square pulse electrical stimuli (200 μs pulse width), delivered through custom-made monopolar tungsten electrodes (Teflon-insulated to the tip of 50 μm diameter). These electrodes enabled a precise placement into the neuronal tissue at the stimulation site and do not interfere with the imaging process (e.g., by producing irritating shadows as observed with other electrodes). A highly localized electrical stimulation was achieved by placing the indifferent electrode far away from the slice in the recording chamber. The electrode used for evocation of EC/DG-input was placed under a binocular on the visually identified PP at distance of 40 μm ($\pm 10 \mu\text{m}$) away from its entry zone into the DG, to avoid direct stimulation of neurons and their dendrites within the ML (Figure 4.2A).

3.7 Chemicals

All salts for the physiological saline solutions were purchased from Sigma-Aldrich. For preparation of stock solutions, AM404 and diazepam were dissolved in DMSO. For pharmacological experiments the corresponding amount of stock solution was diluted in artificial cerebrospinal fluid (ACSF). Therefore, DMSO was present at a maximum concentration of $\leq 0.025\%$ (AM404) and $\leq 0.02\%$ (diazepam). The corresponding amount of DMSO was added during baseline recordings. For a summary see Table (7.1).

3.8 Statistics

Statistical significance was assessed by paired- and unpaired t-tests when appropriate. All tests were run in SigmaStat 3.5 (Systat Software; Chicago; USA) and differences were considered significant if $p < 0.05$. Data are given as mean \pm s.e.m.

Chapter 4

Results

This work is a further implementation of a recently developed voltage-sensitive dye imaging (VSDI) assay in mouse brain slices (see Material and Methods 3; Stepan et al., 2012; Stepan et al., 2015b). This high-speed optical approach allows real-time recording of activity patterns in large/meso-scale neuronal networks and here, in particular, the investigation of activity waves across the entire hippocampal trisynaptic circuit ("HTC-Waves"; Figures 4.1; 4.3; Stepan et al., 2012; Stepan et al., 2015b).

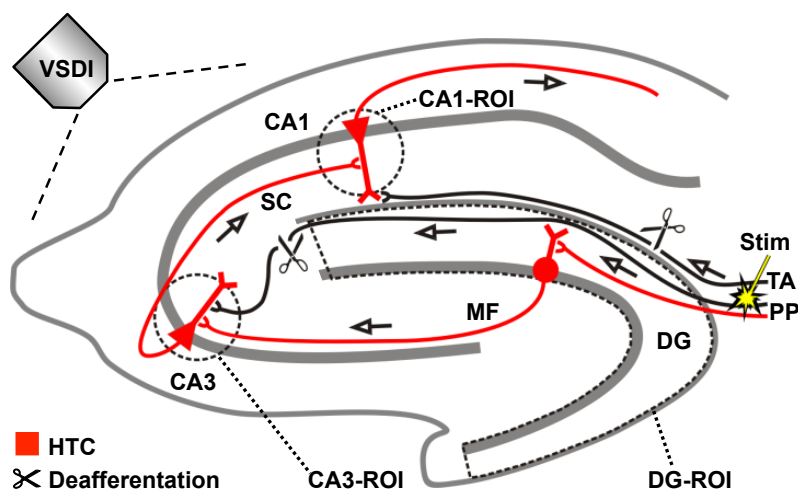


Fig. 4.1. Experimental setup for recordings of polysynaptic activity flow through the HTC network. Arrangement used for experiments shown in Figures (4.3 - 4.8). Abbreviations: MF, mossy fiber; PP, perforant path; ROI, region of interest; SC, Schaffer collateral; Stim, extracellular electrical stimulation; TA, temporoammonic pathway (adapted from Stepan et al., 2015b).

HTC-Waves were triggered by theta-frequency stimulation trains of perforant path fibers (PP), in the following EC/DG-input, mimicking synchronous theta-rhythmical spiking of entorhinal cortex (EC) layer II neurons (Mizuseki et al., 2009; Quilichini et al., 2010; Burgalossi et al., 2011; Stepan et al., 2012; Stepan et al., 2015b). Such activity in the entorhinal-hippocampal system is physiologically highly relevant, because of its major role in complex cognitive functions in mammals, including episodic and spatial memory

(Buzsàki, 2002; Hafting et al., 2005; Rutishauser et al., 2010). Moreover, EC/DG-input in the theta range most effectively passes filter mechanisms associated with the hippocampal trisynaptic circuit (HTC; Stepan et al., 2012; Stepan et al., 2015a). PP-fibers synapse on dendrites of DG principle cells (granule cells) which subsequently give rise to mossy-fibers, the anatomically most prominent non-commissural/associational innervation of CA3 pyramidal cells. To study "pure" activity propagations through the downstream HTC-network, PP fibers that directly innervate areas CA3, CA2 and CA1 (Watson et al., 2011; Kohara et al., 2014), were micro-dissected via specific cuts in all experiments (Figures 3.1, 4.1, 4.2A). As VSDI measure of neuronal activity, "regions of interest" (ROI)-extracted fast, depolarization-mediated imaging signals (FDSs) were used (Figures 4.1, 4.2A, 4.3; Tominaga et al., 2000; Airan et al., 2007; Refojo et al., 2011; Stepan et al., 2012).

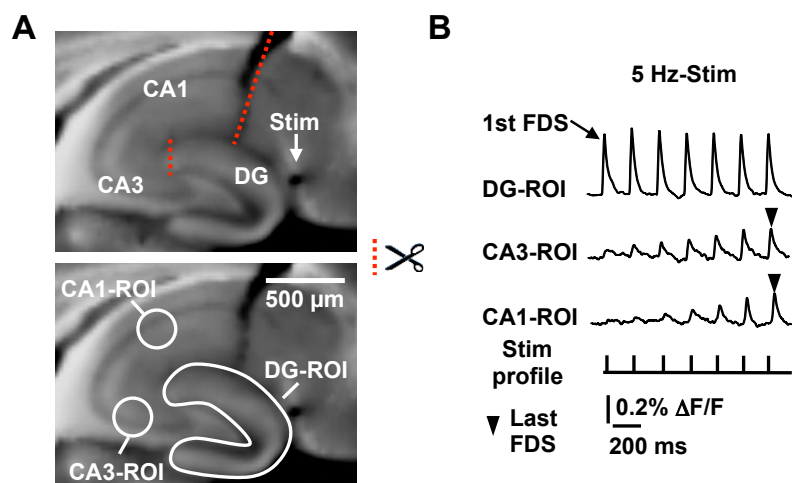


Fig. 4.2. Anatomical position of ROIs and experimental protocol. (A) Illustration of ROI positions and deafferentations in relation to important landmarks in the HIP. (B) Depiction of ROI-extracted fast, depolarization-mediated imaging signals (FDSs), which reflect a compound signal from all stained neuronal membranes, but mainly derive from neuronal action potentials and glutamatergic excitatory postsynaptic potentials (EPSPs). Note the typically increasing CA3 signals and the delayed occurrence of CA1-FDSs, which predominantly result from frequency facilitation of neurotransmission at mossy fiber synapses onto CA3 pyramidal neurons (Nicoll and Schmitz, 2005). Abbreviations: SL, stratum lucidum; SR, stratum radiatum.

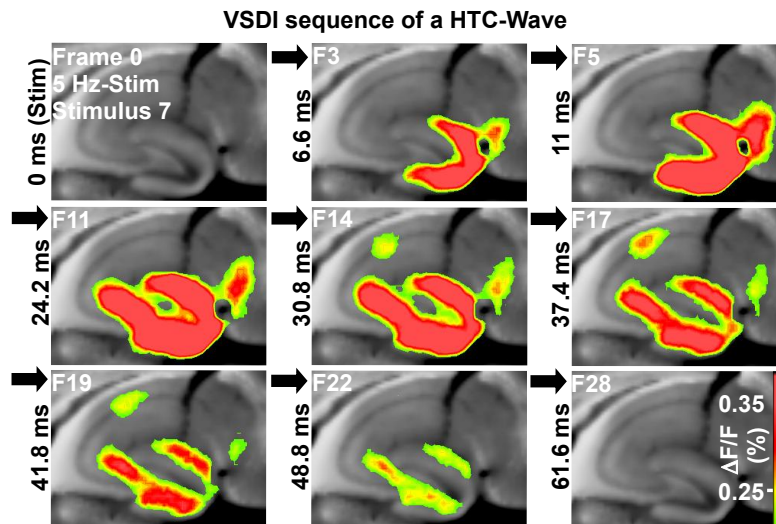


Fig. 4.3. Hippocampal activities in response to 5 Hz EC/DG-input. VSDI filmstrip of a submaximal HTC-Wave evoked by theta-frequency (5 Hz) electrical stimulation train of the PP (stimulus 7). Only selected imaging frames are shown (sampling time was 2.2 ms). Warmer colors represent higher values of the fractional change in fluorescence ($\Delta F/F$) of the voltage-sensitive dye and, thus, stronger neuronal activity.

4.1 Opposing effects of diazepam and AM404 on HTC-Waves

Previous results show that HTC-Waves provide a valuable assay for studying drug effects on polysynaptic activity flow through the classical input/output circuit of the HIP (Stepan et al., 2012; Stepan et al., 2015b). Consistently, theta-frequency stimulus trains applied to the PP containing 7 pulses every 2 min, were suited to conduct stable baseline recordings of HTC-Waves (Figures 4.2, 4.4; Stepan et al., 2015b). The number of stimuli was held constant within an experiment and as a final measure of DG, CA3, and CA1 activity levels, the mean of FDS out of three consecutive acquisitions was used and paired t-tests were employed to determine differences of FDSs at minutes 0 to 18 vs. minutes 42 to 60. Electrical stimulation intensity was set (15-35 V), to obtain CA1-FDS ranging within 0.1 to 0.3 % $\Delta F/F$ (Stepan et al., 2015b). Applying these settings, control experiments with DMSO (solvent of diazepam and AM404) revealed a slight decrease of FDS amplitudes in all hippocampal subregions (significant in the DG; Figure 4.4). To avoid underestimation (AM404) or overestimation (diazepam) of drug effects the corresponding percentage of decrease (DG, $-5.6 \pm 1\%$; CA3, $-5.5 \pm 2\%$; CA1, $-5.5 \pm 2\%$) was added in subsequent experiments.

Benzodiazepines (BDZs) like diazepam are widely used for acute symptom relieve in patients suffering from SRPDs, but simultaneously impair cognitive function in humans and animals, partly, due to their potentiating effect on GABA_A receptor function in the HIP (Shimizu et al., 1998; Chouinard, 2004). In line with this, and, consistent with previous data (Stepan et al., 2012), bath applied diazepam rapidly decreased DG-, CA3-, and CA1-FDSs (Figure 4.5).

Substantial evidence has accumulated, implicating the endocannabinoid system (ECS) to be involved in the pathophysiology of SRPDs and all its components are highly expressed

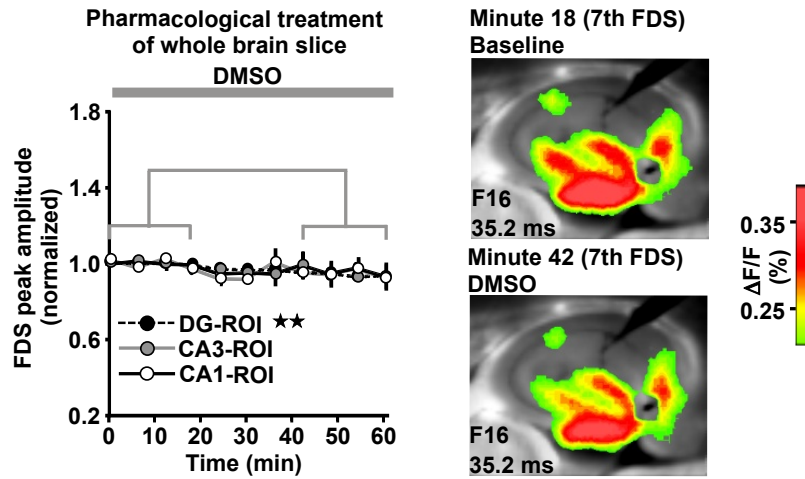


Fig. 4.4. DMSO effect on HTC-Waves. DMSO (0.025%) decreases FDSs in the DG ($t_7 = -5.4$, $p = 0.001$, paired t -test), but has no significant effect in areas CA3 and CA1 ($n = 8$ slices/4 mice). ** $p < 0.01$.

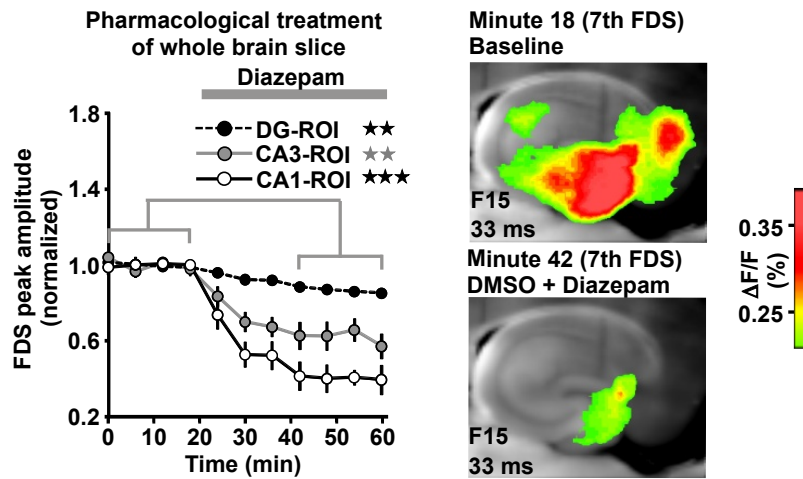


Fig. 4.5. Diazepam effect on HTC-Waves. Diazepam ($1\mu M$) rapidly decreases FDSs in the DG ($t_5 = -6.6$, $p = 0.001$, paired t -test) and areas CA3 ($t_5 = 5.0$, $p = 0.004$, paired t -test) and CA1 ($t_5 = -8.6$, $p < 0.001$; paired t -test) ($n = 6$ slices/5 mice). ** $p < 0.01$, *** $p < 0.001$.

by excitatory and inhibitory neurons in the HIP (Marsicano and Lutz, 1999; Micale et al., 2013). Moreover previous research found anxiolytic- and antidepressant effects of ECS-modulators in rodents, which was associated with less pronounced impairment, or even enhanced amnestic functions (Mangieri and Piomelli, 2007; Riebe et al., 2012; Micale et al., 2017). In line with that, and in contrast to diazepam, the endocannabinoid (eCB) reuptake inhibitor/degradation blocker AM404 (Beltramo et al., 1997) rapidly amplified CA3-, and CA1-FDSs (Figure 4.6).

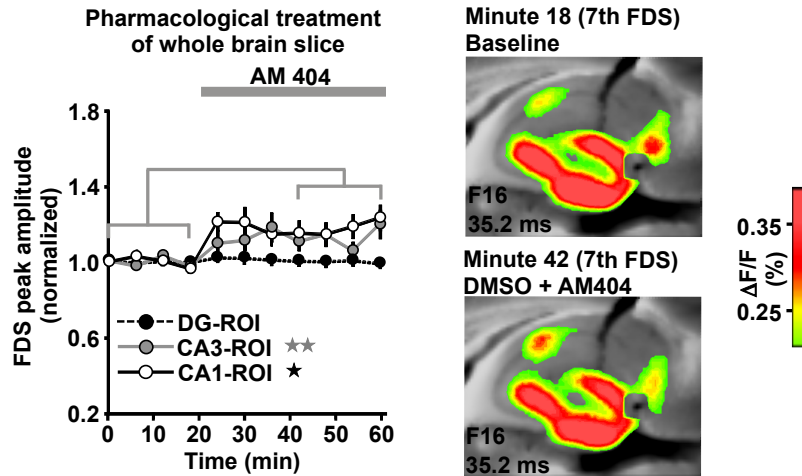


Fig. 4.6. AM404 effect on HTC-Waves. AM404 ($10\mu\text{M}$) rapidly amplifies FDSs in areas CA3 ($t_{(7)} = 3.6$, $p = 0.009$, paired t -test) and CA1 ($t_{(7)} = 3.5$, $p = 0.010$, paired t -test), but not in the DG ($n = 8$ slices/8 mice). * $p < 0.05$, ** $p < 0.01$.

4.2 AM404 effects are mediated by D1R positive neurons

There is potentially a wide range of cellular mechanisms underlying the enhancing effects of AM404 on HTC-Waves. AM404 facilitates eCB signaling and is a potent activator (full agonist) of TRPV1 channels (Beltramo et al., 1997; Beltramo and Piomelli, 2000; De Petrocellis et al., 2000; Zygmunt et al., 2000; Pertwee, 2015). Pilot-experiments using the CB1R antagonist/inverse agonist rimonabant (SR141716) and the TRPV1 antagonist SB363791 revealed that these substances exert strong effects on hippocampal network activity, which somehow hampered a more detailed pharmacological dissection of AM404 effects. Experiments with conditional CB1R-KO mice lacking CB1Rs on forebrain GABAergic, glutamatergic and dopaminergic neurons support the hypothesis that different neuronal subpopulations might be involved in the cellular, molecular and behavioral effects of eCB and ECS-modulators (Marsicano et al., 2003; Monory et al., 2007; Haring et al., 2012; Llorente-Berzal et al., 2015). More specifically, recently obtained data suggest CB1Rs on D1R positive neurons to be critically involved in HIP-dependent AM404 effects on specific learning tasks (Micale et al., 2017). Therefore, AM404 was tested in mice lacking CB1Rs on D1R receptor containing neurons (D1R-CB1R-KO) and control littermates (D1R-CB1R-WT). Bath application of AM404 to slices from D1R-CB1R-KO mice had no effect on DG-, CA3-, and CA1-FDSs, while AM404 again rapidly elevated HTC-Waves in D1R-CB1R-WT mice (Figure 4.7). This shows that CB1R expression on D1R receptor positive forebrain neurons is essential for AM404 effects on hippocampal network activity.

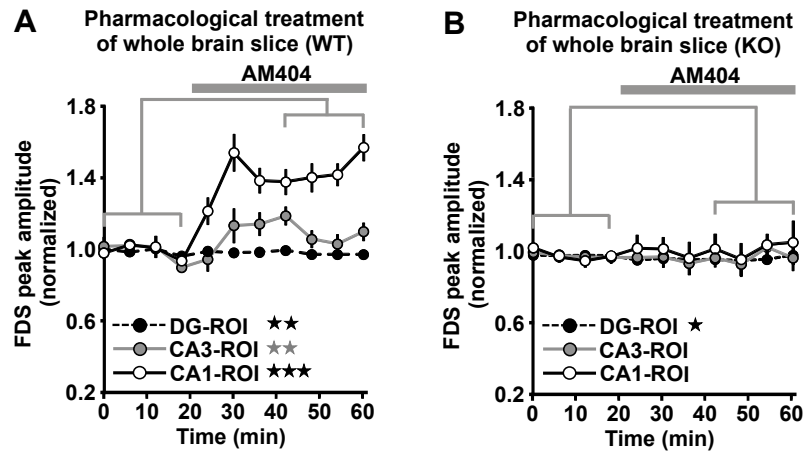


Fig. 4.7. CB1Rs on D1R positive neurons mediate AM404 effects. (A, B) AM404 ($10\mu\text{M}$) effects are present in D1R-CB1R-WT mice ((A) DG: $t_{(5)} = 4.3$, $p = 0.008$; CA3: $t_{(5)} = 4.7$, $p = 0.005$; CA1: $t_{(5)} = 11.4$, $p < 0.001$; paired t -tests; $n = 6$ slices/6 mice), but not in CB1R-D1R-KO mice, except for the DG ((B) DG: $t_{(5)} = 2.8$, $p = 0.032$; paired t -test; $n = 7$ slices/7mice). * $p < 0.05$, ** $p < 0.01$, *** $p < 0.001$.

4.3 Hippocampal subregion specific drug effects

Next, it was tested if drug induced enhanced/weakened HTC-Waves result from increased/ decreased neuronal activity in both, area CA3 and CA1. Further analysis of the data revealed that the amplitude of CA1-FDSs linearly increased with the amplitude of CA3-FDSs (data from $N = 4$ DMSO experiments, Figure 4.8A). CA3/CA1 activity ratios were calculated for all experiments to assess drug effects in CA subregions. These ratios were calculated by dividing the mean amplitude value of the last three CA3-FDSs by the mean amplitude value of the last three CA1-FDSs within a recording sequence (Stepan et al., 2015b). AM404 reduced CA3/CA1 activity ratios in D1R-CB1R-WT animals but not in C57BL/6N mice while diazepam had the opposite effect (Figure 4.8B). No change in CA3/CA1 activity ratios was found in DMSO experiments and in D1R-CB1R-KO mice (Figure 4.8B). These findings suggest that drug effects on HTC-Waves originated in most cases from impaired/enhanced neurotransmission in both, area CA3 and area CA1.

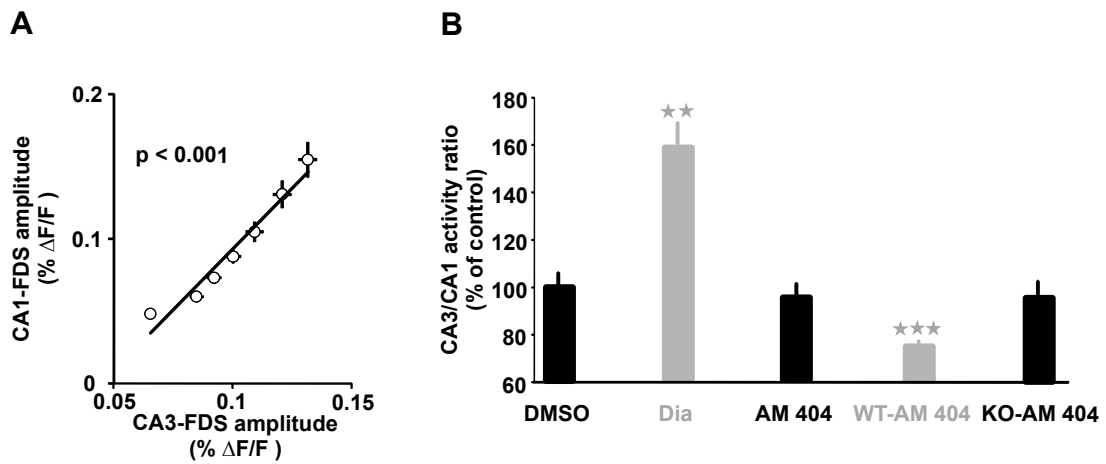


Fig. 4.8. CA3/CA1 activity ratios are drug specific (A) In slices from control experiments, the amplitude of CA1-FDSs linearly increased with the amplitude of CA3-FDSs. Data were obtained by averaging the CA1- and CA3-FDS amplitude values for electrical stimulus 1, 2, 3, ..., 7 over $n = 4$ experiments performed in control (DMSO) mice, in which the electrical stimulation intensity was set to obtain CA1-FDSs ranging within 0.1 to 0.3 % $\Delta F/F$ during baseline recordings. (B) Relative change in CA3/CA1 activity ratios in the experiments with DMSO (Figure 4.4), diazepam (Figure 4.5; $t_{(5)} = 6.2$, $p = 0.002$; unpaired- t -test) and AM404 (Figures 4.6 and 4.7; D1R-CB1R-WT: $t_{(5)} = -18.1$, $p < 0.001$; unpaired t -test). ** $p < 0.01$ *** $p < 0.001$.

Chapter 5

Discussion

The present data illustrates a dichotomy between the ability of diazepam, a widely prescribed drug to treat the symptoms of SRPDs (Rudolph and Knoflach, 2011) and AM404, an endocannabinoid signaling enhancer with antidepressant and anxiolytic potential (Beltramo et al., 1997; Adamczyk et al., 2008; Riebe et al., 2012), to modulate the activity flow through the the HIP. Diazepam impaired activity propagations through the hippocampal trisynaptic circuit (HTC-Waves) in the DG and in CA regions (Stepan et al., 2015b), while AM404 caused an amplification of HTC-Waves in areas CA3 and CA1. The rapid facilitation of HTC-Waves after AM404 application supports previous findings suggesting a prominent role for the eCB system in the regulation of hippocampal homeostasis and excitability (Marsicano et al., 2003; Péterfi et al., 2012; Stempel et al., 2016). This altered excitability in a brain area ascribed a pivotal role in learning and memory and the pathophysiology of SRPDs (Burgess et al., 2002; Berton and Nestler, 2006), in combination with previous results, indicating that diazepam severely disrupts cognitive processes while AM404 facilitates acquisition of new information (Buffett-Jerrott and Stewart, 2002; Micale et al., 2017), further supports the hypothesis that drugs, which impact diverse cellular- and molecular processes, change behavioral output by a common "circuit-level" mechanism (Castrén, 2005; Airan et al., 2007; Stepan et al., 2015b). In line with that, Stepan et al. (2015b) found that various antidepressants (ADs), belonging to different chemical/functional classes, and drugs with antidepressant potential like brain-derived neurotrophic factor (BDNF), ketamine and lithium enhance HTC-Waves at clinically relevant concentrations, whereas substances with no antidepressant potential and stress weaken HTC-Waves (Stepan et al., 2015b). Similar studies using VSDI to map diverse drug-, or genetically induced cellular alterations, also found specific circuit-level endophenotypes supporting the view that VSDI might be useful to narrow the gap between cellular/ molecular processes and behavioral outcome (Airan et al., 2007; von Wolff et al., 2011; Refojo et al., 2011; Kim et al., 2012; Avrabos et al., 2013; Ikrar et al., 2013; Stepan et al., 2015b).

Like most medications commonly used to treat SRPDs (e. g. ADs), AM404 has a polypharmacological profile causing multifarious molecular-, cellular-, and behavioral actions by itself, including enhanced eCB-signaling (see Introduction 1.1; Beltramo et al., 1997; De Petrocellis et al., 2000; Zygmunt et al., 2000; Glaser et al., 2003; Hogestatt et al., 2005; Wiskerke et al., 2012; Kano, 2014; Pertwee, 2015; Micale et al., 2017; Busquets Garcia et al., 2016). Substances affecting a variety of targets are sometimes called "dirty" or "promiscuous" drugs and were supposed to have a better efficacy (Frantz, 2005; Marks et al., 2008), but delineating their exact mode of action has proven difficult (Moreira et al., 2012; Busquets Garcia et al., 2016). AM404 elevates plasmatic levels of AEA either by reuptake inhibition (Beltramo et al., 1997; Fu et al., 2012) and/or by blocking degradation enzymes like FAAH-1 (Glaser et al., 2003; Fowler, 2013; Glaser et al., 2005). Moreover, AM404 elevates 2-AG levels in the brain (Hajos et al., 2004). Pharmacokinetic differences between AEA and 2-AG could influence AM404-mediated effects (Hill et al., 2009). AEA binds with high affinity to CB1Rs with K_i values of approximately 50-1000 nM but is a partial agonist resulting in poor efficacy. By contrast, 2-AG binds to CB1Rs with K_i values of approximately 1-10 μ M, but is a potent, full agonist inducing a robust activation of downstream signaling cascades (Hill et al., 2009). Therefore, it was suggested that AEA mediates tonic activation of CB1R receptors while 2-AG becomes activated during activity-induced changes in synaptic transmission (Hill et al., 2009).

In general, the ECS predominantly functions by reducing neural excitability at GABAergic, glutamatergic, serotonergic, dopaminergic, and cholinergic neurons through presynaptic inhibition of transmitter release and by eCB-dependent forms of short- and long-term depression via CB1Rs and CB2Rs (Kano, 2014; Morena et al., 2016; Stempel et al., 2016). Therefore, it is conceivable that AM404 exerts a depressing effect on neurotransmission and thus, HTC-Waves. However, distribution of CB1R is not equal across neuronal populations in the HIP. GABAergic axon terminals express high levels of CB1Rs, especially cholecystokinin (CCK) coexpressing interneurons, while expression levels in glutamatergic neurons are considerably low (Katona et al., 1999; Hu and Mackie, 2015; Pertwee, 2015). Because intrahippocampal information flow through glutamatergic synaptic transmission is tightly regulated by GABAergic interneurons, their silencing could result in disinhibition of local (Katona et al., 1999) and large/mesoscale neuronal networks Figure (4.5). Moreover, AM404 and AEA are potent activators of TRPV1 (De Petrocellis et al., 2000; Zygmunt et al., 2000), a non-selective cation channel, which mediates specific forms of synaptic plasticity in the HIP (Marsch et al., 2007; Gibson et al., 2008), complemented by numerous studies of eCB-driven modulation of neuronal excitability and plasticity (Carta et al., 2014; Stempel et al., 2016). In conclusion, this underlines the importance of high-speed optical approaches to leave extrapolation of cellular/molecular effects onto network function, and to directly obtain pharmacological "net" effects in the mammalian brain (Airan et al., 2007; Stepan et al., 2012; Avrabos et al., 2013; Stepan et al., 2015a; Stepan et al., 2015b).

The ECS is frequently mentioned in connection with alterations of learning and memory a key symptom of SRPDs, which likely involves the HIP. But, how exactly are network patterns in the HIP related to learning and memory? HTC-Waves, triggered by 5 Hz EC/DG-input have been shown to induce high-frequency firing (>100 Hz) of CA3 pyramidal neurons with subsequent induction of NMDA receptor-dependent CA1 long-term potentiation (LTP) within a few seconds (Stepan et al., 2012). This neuroplastic phenomenon is a compelling and extensively used experimental model for a cellular correlate that underlies specific types of learning and memory, and the observation that CA1 LTP also naturally occurs in the brain suggests that it is required for some forms of explicit learning in mammals (Gruart et al., 2006; Whitlock et al., 2006; Ho et al., 2011). Here, a reduced number of stimuli was used which allows stable baseline recordings prevents the induction long-term synaptic changes (Stepan et al., 2012; Stepan et al., 2015b). But, weakened activity propagations through the HTC should be less effective in the induction of CA1 LTP. Accordingly diazepam attenuates induction of CA1 LTP *in vitro* and *in vivo* most likely via the BDZ site of GABA_A-receptors resulting in potentiation of inhibitory neurotransmission (del Cerro et al., 1992; Mori et al., 2001; Tokuda et al., 2010). Moreover, extensive research in animals and humans suggest BDZ to impair HIP-dependent cognitive abilities like the acquisition of reference and explicit memories (Timic et al., 2013; Buffett-Jerrott and Stewart, 2002). This is of particular interest because drug administration in combination with psychotherapy represents the gold standard in the treatment of many SRPDs (Association, 2013), which might be less effective when patients receive BDZs (Guina et al., 2015). Interestingly, exposure of mice to chronic stress parallels the effects of BDZ in the HIP (Stepan et al., 2015b). Chronic stress causes various molecular, cellular and circuit changes in the HIP and alters the ECS throughout the brain (Sapolsky et al., 1986; Lutz et al., 2015). Although this clearly differentiates the mechanisms by which stress and diazepam effect HTC-Waves, they share the ability to reduce cognitive performance, which might involve a common endophenotype, namely, reduced activity percolations through the HTC.

In contrast to diazepam, AM404 enhance HTC-Waves suggesting a lower threshold for the induction of CA1 LTP and thus, facilitation of HIP-dependent memories. In line with that, the AD fluoxetine, which also facilitates HTC-Waves, lowers the threshold for LTP at a clinically relevant concentration (Stepan, 2015; Stepan et al., 2015b). On the cellular level contradicting results were obtained regarding the ability of AM404, eCB agonists and eCB to influence CA1 LTP induction (Terranova et al., 1995; Stella et al., 1997; Abush and Akirav, 2010; Basavarajappa et al., 2014). Abush and Akirav (2010) found that eCB agonists, including AM404 impaired CA1 LTP induction. Likewise results were obtained for the two most studied eCB AEA and 2-AG (Stella et al., 1997; Terranova et al., 1995; Basavarajappa et al., 2014). However, it is important to note, that most research on LTP *in vitro* is performed in isolated, monosynaptic pathways and not on the network level with a physiological stimulation protocol (Buzsàki, 1988; Abush and Akirav, 2010; Stepan et al., 2012). On the behavioral level, experiments using eCB or ECS modulators obtained different results depending on the applied drug,

injection side and, most importantly, the test paradigm used (Abush and Akirav, 2010; Riebe et al., 2012; Micale et al., 2017). Recently, Micale et al. (2017) found that learning about the safety of an environment (i.e., safety learning) allow mice to overcome their avoidance behavior in a step-down avoidance task, a process that was impaired by CA1 injections of diazepam and facilitated by CA1 injections of AM404 Micale et al. (2017). Interestingly, AM404 effects were also absent in D1R-CB1R-KO mice, which together with the present data suggests, that enhanced eCB signaling promotes safety learning by facilitating activity propagation through the HTC (Micale et al., 2017). Furthermore, the behavioral data support the hypothesis that cannabinoid agonists facilitate emotional memory like extinction of inhibitory avoidance, and impair nonemotional memory like spatial navigation (Abush and Akirav, 2010). But, Abush and Akirav (2010) and others emphasize that such simplified perspective underestimates the complexity of how cannabinoids modulate memory processes (Abush and Akirav, 2010; Lutz et al., 2015), supporting the present findings in the dorsal HIP, an anatomical part, mainly involved in nonemotional processes (Fanselow and Dong, 2010).

Enhanced activity flow through the HTC and the associated increased output from area CA1 in response to AM404 treatment, might not only be pivotal for cognitive processes (Stepan et al., 2015a), but also represents a putative mechanism for the regulation of the neuroendocrine stress response mediated by the hypothalamic-pituitary-adrenal (HPA)-axis (Radley, 2012). HPA-axis dysfunction with hypersecretion of stress-hormones is thought to be involved in the etiology of SRPDs and is found in up to 50% of depressed patients (Holsboer, 2000; de Kloet et al., 2005). Especially the ventral HIP is part of a multi-synaptic circuit, relevant for HPA-axis regulation and thus the amount of circulating stress-hormones (Morena et al., 2016). A wealth of research shows that chronic stress and elevated stress-hormones dampen HIP activity, causing a disruption of the HIP-dependent negative feedback control over the HPA-axis (Watanabe et al., 1992; Radley, 2012), and likely promoting a vicious circle and further exacerbation of functional impairment (Sapolsky et al., 1986). Excitatory hippocampal output has been shown to activate inhibitory neurons in the bed nucleus of the stria terminalis which subsequently target CRH-producing parvocellular neurons in the hypothalamus (Radley, 2012; Kondoh et al., 2016). Accordingly, HPA-axis hyperactivity is dampened by ADs (Holsboer and Barden, 1996), which share their circuit-level effect on HTC-Waves with AM404 (Stepan et al., 2015b). Both enhance hippocampal output and thereby might counteract stress induced impairment of hippocampal function and HPA-axis disinhibition (Radley, 2012; Stepan et al., 2015b). This overlap in the effects of AM404 and ADs on hippocampal network dynamics (Stepan et al., 2015b), in combination with the pronounced interactions between stress and the eCB (Morena et al., 2016), supports the hypothesis that increased eCB signaling might contribute to the mechanism by which ADs modulate HPA-axis function (Hill et al., 2009). However, for reasons of methodology, HTC-Waves were evoked in dorsal or intermediate parts of the HIP, so that future studies have to examine

if the present results also apply for the ventral hippocampus (see also Introduction (1.2)).

Surprisingly, AM404 induced facilitation of HTC-Waves was absent in conditional D1R-CB1R-KO mice. Expression of D1R has been shown in all hippocampal subregions (Gangarossa et al., 2012) and their activation modulates basic neurotransmission and synaptic plasticity in brain slices (Otmakhova and Lisman, 1996; Kobayashi and Suzuki, 2007; Ito and Schuman, 2007), as well as learning and memory in behaving animals (Sarinana and Tonegawa, 2016). Although, coexpression of CB1Rs with D1Rs has not been shown in the HIP so far (Hermann et al., 2002; Monory et al., 2007), the present results ascribe D1R-CB1R coexpressing neurons a pivotal role in mediating network effects of AM404 in the HIP. However, further studies combining anatomical, molecular, cellular and functional methods will be necessary to clarify the existence and the functional properties of D1R/CB1R coexpressing neurons in the HIP.

According to a recent study (Stepan et al., 2015b), a detailed analysis of the data revealed that diazepam elevates the CA3/CA1 activity-ratio in the HIP, supporting the idea of drug-related endophenotypes. The data also suggests drug effects in both, area CA3 and area CA1, expressing high GABA_A-receptor expression levels across the entire DG-CA-axis (Rudolph and Knoflach, 2011). This is also true for AM404 (enhanced HTC-Waves = reduced CA3/CA1 activity ratio; Stepan et al., 2015b). But, while the CA3/CA1 activity ratio in D1R-CB1R-WT is reduced, it is unchanged in C57BL/6N animals (Figure 4.8). This discrepancy compared to a previous study (Stepan et al., 2015b), could result from differences in age, genetic background, or from manifold methodological issues, such as evoked neuronal activity levels, conservation of intrahippocampal connections and vitality of the slice, all of which are pivotal for the induction of polysynaptic activity flow (Bischofberger et al., 2006; Stepan et al., 2012). In contrast to previous work using the HTC-Wave assay (Stepan et al., 2012; Stepan et al., 2015b), activity levels in CA1 do not clearly exceed CA3 FDSs, which might account for missing effects of AM404 on CA3/CA1 activity ratio in C57BL/6N mice.

In summary, VSDI was used to show how a complex pattern of drug induced cellular/molecular actions translate into a neuronal network response (Busquets Garcia et al., 2016). The stereotyped effects of AM404 and diazepam, support the idea of shared, circuit-level drug effects, to counteract disease-related dysfunction of the hippocampal network (Stepan et al., 2015a; Stepan et al., 2015b). The HTC-Wave assay combined with classical electrophysiology and cell type-specific silencing/activation of neuronal subpopulations (optogenetics, "all optical approach"; Zhang et al., 2010; Emiliani et al., 2015), should be used in future experiments to improve knowledge about ECS function and its role in relevant neuronal network patterns like excitation/inhibition balance (Yizhar et al., 2011).

Chapter 6

Bibliography

- Abush H, Akirav I (2010) Cannabinoids modulate hippocampal memory and plasticity. *Hippocampus* 20:1126–38.
- Adamczyk P, Golda A, McCreary AC, Filip M, Przegalinski E (2008) Activation of endocannabinoid transmission induces antidepressant-like effects in rats. *J Physiol Pharmacol* 59:217–28.
- Airan RD, Meltzer LA, Roy M, Gong Y, Chen H, Deisseroth K (2007) High-speed imaging reveals neurophysiological links to behavior in an animal model of depression. *Science* 317:819–23.
- Alger BE, Kim J (2011) Supply and demand for endocannabinoids. *Trends Neurosci* 34:304–15.
- Amaral DG (1993) Emerging principles of intrinsic hippocampal organization. *Curr Opin Neurobiol* 3:225–9.
- Amaral DG, Scharfman HE, Lavenex P (2007) The dentate gyrus: fundamental neuroanatomical organization (dentate gyrus for dummies). *Dentate Gyrus: A Comprehensive Guide to Structure, Function, and Clinical Implications* 163:3–22.
- Amaral DG, Witter MP (1989) The three-dimensional organization of the hippocampal formation: A review of anatomical data. *Neuroscience* 31:571–91.
- Andersen P, Morris R, Amaral D, Bliss T, O'Keefe J (2006) *The Hippocampus Book*. New York, NY: Oxford University Press.
- Association A (2013) *Diagnostic and Statistical Manual of Mental Disorders (DSM-5®)*. American Psychiatric Publishing.
- Avrabet C, Sotnikov SV, Dine J, Markt PO, Holsboer F, Landgraf R, Eder M (2013) Real-time imaging of amygdalar network dynamics in vitro reveals a neurophysiological link to behavior in a mouse model of extremes in trait anxiety. *J Neurosci* 33:16262–7.
- Backus AR, Bosch SE, Ekman M, Grabovetsky AV, Doeller CF (2016) Mnemonic convergence in the human hippocampus. *Nat Commun* 7:11991.
- Baker BJ, Kosmidis EK, Vucinic D, Falk CX, Cohen LB, Djuricic M, Zecevic D (2005) Imaging brain activity with voltage- and calcium-sensitive dyes. *Cell Mol Neurobiol* 25:245–82.

- Bandelow B, Lichte T, Rudolf S, Wiltink J, Beutel ME (2014) The diagnosis of and treatment recommendations for anxiety disorders. *Dtsch Arztebl Int* 111:473–80.
- Basavarajappa BS, Nagre NN, Xie S, Subbanna S (2014) Elevation of endogenous anandamide impairs LTP, learning, and memory through CB1 receptor signaling in mice. *Hippocampus* 24:808–18.
- Bear MFC BW, Paradiso MA (2016) *Neuroscience: exploring the brain* Philadelphia: Wolters Kluwer.
- Beltramo M, Piomelli D (2000) Carrier-mediated transport and enzymatic hydrolysis of the endogenous cannabinoid 2-arachidonylglycerol. *Neuroreport* 11:1231–5.
- Beltramo M, Stella N, Calignano A, Lin SY, Makriyannis A, Piomelli D (1997) Functional role of high-affinity anandamide transport, as revealed by selective inhibition. *Science* 277:1094–7.
- Berton O, Nestler EJ (2006) New approaches to antidepressant drug discovery: Beyond monoamines. *Nat Rev Neurosci* 7:137–51.
- Bischofberger J, Engel D, Li L, Geiger JR, Jonas P (2006) Patch-clamp recording from mossy fiber terminals in hippocampal slices. *Nature Protocols* 1:2075–81.
- Buffett-Jerrott SE, Stewart SH (2002) Cognitive and sedative effects of benzodiazepine use. *Curr Pharm Des* 8:45–58.
- Burgalossi A, Herfst L, von Heimendahl M, Förste H, Haskic K, Schmidt M, Brecht M (2011) Microcircuits of functionally identified neurons in the rat medial entorhinal cortex. *Neuron* 70:773–86.
- Burgess N, Maguire EA, O'Keefe J (2002) The human hippocampus and spatial and episodic memory. *Neuron* 35:625–41.
- Busquets Garcia A, Soria-Gomez E, Bellocchio L, Marsicano G (2016) Cannabinoid receptor type-1: breaking the dogmas. *F1000Res* 5.
- Buzsàki G (1988) Polysynaptic long-term potentiation: A physiological role of the perforant path-CA3/CA1 pyramidal cell synapse. *Brain Res* 455:192–5.
- Buzsàki G (2002) Theta oscillations in the hippocampus. *Neuron* 33:325–40.
- Caddy C, Amit BH, McCloud TL, Rendell JM, Furukawa TA, McShane R, Hawton K, Cipriani A (2015) Ketamine and other glutamate receptor modulators for depression in adults. *Cochrane Database Syst Rev* 9:CD011612.
- Cai X, Kallarackal AJ, Kvarita MD, Goluskin S, Gaylor K, Bailey AM, Lee HK, Haganir RL, Thompson SM (2013) Local potentiation of excitatory synapses by serotonin and its alteration in rodent models of depression. *Nat Neurosci* 16:464–72.
- Canepari M, Zecevic D (2010) *Membrane potential imaging in the nervous system: Methods and applications*. New York, NY: Springer.
- Carlson GC, Coulter DA (2008) In vitro functional imaging in brain slices using fast voltage-sensitive dye imaging combined with whole-cell patch recording. *Nature Protocols* 3:249–55.
- Carta M, Lanore F, Rebola N, Szabo Z, Da Silva SV, Lourenço J, Verraes A, Nadler A, Schultz C, Blanchet C, Mülle C (2014)

- Membrane lipids tune synaptic transmission by direct modulation of presynaptic potassium channels. *Neuron* 81:787–99.
- Cascio MG, Marini P (2015) Biosynthesis and Fate of Endocannabinoids. *Handb Exp Pharmacol* 231:39–58.
- Castillo PE, Younts TJ, Chavez AE, Hashimoto Y (2012) Endocannabinoid signaling and synaptic function. *Neuron* 76:70–81.
- Castrén E (2005) Opinion - Is mood chemistry? *Nature Reviews Neuroscience* 6:241–246.
- Chávez AE, Chiu CQ, Castillo PE (2010) TRPV1 activation by endogenous anandamide triggers postsynaptic long-term depression in dentate gyrus. *Nat Neurosci* 13:1511–8.
- Chemla S, Chavane F (2010) Voltage-sensitive dye imaging: Technique review and models. *J Physiol Paris* 104:40–50.
- Chouinard G (2004) Issues in the clinical use of benzodiazepines: potency, withdrawal, and rebound. *J Clin Psychiatry* 65 Suppl 5:7–12.
- Claiborne BJ, Amaral DG, Cowan WM (1986) A light and electron microscopic analysis of the mossy fibers of the rat dentate gyrus. *J Comp Neurol* 246:435–58.
- Coleman JA, Green EM, Gouaux E (2016) X-ray structures and mechanism of the human serotonin transporter. *Nature* .
- Daumas S, Ceccom J, Halley H, Francés B, Lassalle JM (2009) Activation of metabotropic glutamate receptor type 2/3 supports the involvement of the hippocampal mossy fiber pathway on contextual fear memory consolidation. *Learn Mem* 16:504–7.
- de Kloet ER, Joëls M, Holsboer F (2005) Stress and the brain: From adaptation to disease. *Nat Rev Neurosci* 6:463–75.
- De Petrocellis L, Bisogno T, Davis JB, Pertwee RG, Di Marzo V (2000) Overlap between the ligand recognition properties of the anandamide transporter and the VR1 vanilloid receptor: inhibitors of anandamide uptake with negligible capsaicin-like activity. *FEBS Lett* 483:52–6.
- deCharms RC (2008) Applications of real-time fMRI. *Nat Rev Neurosci* 9:720–9.
- del Cerro S, Jung M, Lynch G (1992) Benzodiazepines block long-term potentiation in slices of hippocampus and piriform cortex. *Neuroscience* 49:1–6.
- Devane WA, Hanus L, Breuer A, Pertwee RG, Stevenson LA, Griffin G, Gibson D, Mandelbaum A, Etinger A, Mechoulam R (1992) Isolation and structure of a brain constituent that binds to the cannabinoid receptor. *Science* 258:1946–9.
- Di Marzo V (2010) Anandamide serves two masters in the brain. *Nat Neurosci* 13:1446–8.
- Di Marzo V, De Petrocellis L (2012) Why do cannabinoid receptors have more than one endogenous ligand? *Philos Trans R Soc Lond B Biol Sci* 367:3216–28.
- Eklund A, Nichols TE, Knutsson H (2016) Cluster failure: Why fMRI inferences for spatial extent have inflated false-positive rates. *Proc Natl Acad Sci U S A* 113:7900–5.
- Emiliani V, Cohen AE, Deisseroth K, Hausser M (2015) All-Optical Interrogation of Neural Circuits. *J Neurosci* 35:13917–26.

- Fanselow MS, Dong HW (2010) Are the dorsal and ventral hippocampus functionally distinct structures? *Neuron* 65:7–19.
- Fluhler E, Burnham VG, Loew LM (1985) Spectra, membrane binding, and potentiometric responses of new charge shift probes. *Biochemistry* 24:5749–55.
- Fowler CJ (2013) Transport of endocannabinoids across the plasma membrane and within the cell. *FEBS J* 280:1895–904.
- Frantz S (2005) Drug discovery: playing dirty. *Nature* 437:942–3.
- Fu J, Bottegoni G, Sasso O, Bertorelli R, Rocchia W, Masetti M, Guijarro A, Lodola A, Armirotti A, Garau G, Bandiera T, Reggiani A, Mor M, Cavalli A, Piomelli D (2012) A catalytically silent FAAH-1 variant drives anandamide transport in neurons. *Nat Neurosci* 15:64–9.
- Gangarossa G, Longueville S, De Bundel D, Perroy J, Herve D, Girault JA, Valjent E (2012) Characterization of dopamine D1 and D2 receptor-expressing neurons in the mouse hippocampus. *Hippocampus* 22:2199–207.
- Gaoni Y, Mechoulam R (1971) The isolation and structure of delta-1-tetrahydrocannabinol and other neutral cannabinoids from hashish. *J Am Chem Soc* 93:217–24.
- Gibson HE, Edwards JG, Page RS, Van Hook MJ, Kauer JA (2008) TRPV1 channels mediate long-term depression at synapses on hippocampal interneurons. *Neuron* 57:746–59.
- Glaser ST, Abumrad NA, Fatade F, Kaczocha M, Studholme KM, Deutsch DG (2003) Evidence against the presence of an anandamide transporter. *Proc Natl Acad Sci U S A* 100:4269–74.
- Glaser ST, Kaczocha M, Deutsch DG (2005) Anandamide transport: a critical review. *Life Sci* 77:1584–604.
- Grinvald A, Hildesheim R (2004) VSDI: a new era in functional imaging of cortical dynamics. *Nat Rev Neurosci* 5:874–85.
- Gruart A, Muñoz MD, Delgado-García JM (2006) Involvement of the CA3-CA1 synapse in the acquisition of associative learning in behaving mice. *J Neurosci* 26:1077–87.
- Guina J, Rossetter SR, De RB, Nahhas RW, Welton RS (2015) Benzodiazepines for PTSD: A Systematic Review and Meta-Analysis. *J Psychiatr Pract* 21:281–303.
- Hafting T, Fyhn M, Molden S, Moser MB, Moser EI (2005) Microstructure of a spatial map in the entorhinal cortex. *Nature* 436:801–6.
- Hajos N, Kathuria S, Dinh T, Piomelli D, Freund TF (2004) Endocannabinoid transport tightly controls 2-arachidonoyl glycerol actions in the hippocampus: effects of low temperature and the transport inhibitor AM404. *Eur J Neurosci* 19:2991–6.
- Haring M, Guggenhuber S, Lutz B (2012) Neuronal populations mediating the effects of endocannabinoids on stress and emotionality. *Neuroscience* 204:145–58.
- Hashimoto-dani Y, Ohno-Shosaku T, Tanimura A, Kita Y, Sano Y, Shimizu T, Di Marzo V, Kano M (2013) Acute inhibition of diacylglycerol lipase blocks endocannabinoid-mediated retrograde signalling: evidence for on-demand

- biosynthesis of 2-arachidonoylglycerol. *J Physiol* 591:4765–76.
- Hermann H, Marsicano G, Lutz B (2002) Coexpression of the cannabinoid receptor type 1 with dopamine and serotonin receptors in distinct neuronal subpopulations of the adult mouse forebrain. *Neuroscience* 109:451–60.
- Hill MN, Hillard CJ, Bambico FR, Patel S, Gorzalka BB, Gobbi G (2009) The therapeutic potential of the endocannabinoid system for the development of a novel class of antidepressants. *Trends Pharmacol Sci* 30:484–93.
- Hillard CJ, Weinlander KM, Stuhr KL (2012) Contributions of endocannabinoid signaling to psychiatric disorders in humans: genetic and biochemical evidence. *Neuroscience* 204:207–29.
- Ho VM, Lee JA, Martin KC (2011) The cell biology of synaptic plasticity. *Science* 334:623–8.
- Hoffman EJ, Mathew SJ (2008) Anxiety disorders: a comprehensive review of pharmacotherapies. *Mt Sinai J Med* 75:248–62.
- Hogestatt ED, Jonsson BA, Ermund A, Andersson DA, Bjork H, Alexander JP, Cravatt BF, Basbaum AI, Zygmunt PM (2005) Conversion of acetaminophen to the bioactive N-acylphenolamine AM404 via fatty acid amide hydrolase-dependent arachidonic acid conjugation in the nervous system. *J Biol Chem* 280:31405–12.
- Holsboer F (2000) The corticosteroid receptor hypothesis of depression. *Neuropsychopharmacology* 23:477–501.
- Holsboer F (2008) How can we realize the promise of personalized antidepressant medicines? *Nat Rev Neurosci* 9:638–46.
- Holsboer F, Barden N (1996) Antidepressants and hypothalamic-pituitary-adrenocortical regulation. *Endocr Rev* 17:187–205.
- Holsboer F, Gruender G, Benkert O (2012) *Handbuch der Psychopharmakotherapie*. Heidelberg: Springer.
- Hu SS, Mackie K (2015) Distribution of the Endocannabinoid System in the Central Nervous System. *Handb Exp Pharmacol* 231:59–93.
- Iijima T, Witter MP, Ichikawa M, Tomimaga T, Kajiwara R, Matsumoto G (1996) Entorhinal-hippocampal interactions revealed by real-time imaging. *Science* 272:1176–9.
- Ikrar T, Guo N, He K, Besnard A, Levinson S, Hill A, Lee HK, Hen R, Xu X, Sahay A (2013) Adult neurogenesis modifies excitability of the dentate gyrus. *Front Neural Circuits* 7:204.
- Ito HT, Schuman EM (2007) Frequency-dependent gating of synaptic transmission and plasticity by dopamine. *Front Neural Circuits* 1:1.
- Kano M (2014) Control of synaptic function by endocannabinoid-mediated retrograde signaling. *Proc Jpn Acad Ser B Phys Biol Sci* 90:235–50.
- Karayiorgou M, Flint J, Gogos JA, Malenka RC, Genetic, Group NCiPW (2012) The best of times, the worst of times for psychiatric disease. *Nat Neurosci* 15:811–2.

- Katona I, Sperlagh B, Sik A, Kafalvi A, Vizi ES, Mackie K, Freund TF (1999) Presynaptically located CB1 cannabinoid receptors regulate GABA release from axon terminals of specific hippocampal interneurons. *J Neurosci* 19:4544–58.
- Kessler RC, Berglund P, Demler O, Jin R, Merikangas KR, Walters EE (2005) Lifetime prevalence and age-of-onset distributions of DSM-IV disorders in the National Comorbidity Survey Replication. *Arch Gen Psychiatry* 62:593–602.
- Kim CS, Chang PY, Johnston D (2012) Enhancement of Dorsal Hippocampal Activity by Knockdown of HCN1 Channels Leads to Anxiolytic- and Antidepressant-like Behaviors. *Neuron* 75:503–16.
- Klar TA, Hell SW (1999) Subdiffraction resolution in far-field fluorescence microscopy. *Opt Lett* 24:954–6.
- Klausberger T, Somogyi P (2008) Neuronal diversity and temporal dynamics: the unity of hippocampal circuit operations. *Science* 321:53–7.
- Klengel T, Binder EB (2015) Epigenetics of Stress-Related Psychiatric Disorders and Gene x Environment Interactions. *Neuron* 86:1343–57.
- Kobayashi K, Suzuki H (2007) Dopamine selectively potentiates hippocampal mossy fiber to CA3 synaptic transmission. *Neuropharmacology* 52:552–61.
- Kohara K, Pignatelli M, Rivest AJ, Jung HY, Kitamura T, Suh J, Frank D, Kajikawa K, Mise N, Obata Y, Wickersham IR, Tonegawa S (2014) Cell type-specific genetic and optogenetic tools reveal hippocampal CA2 circuits. *Nat Neurosci* 17:269–79.
- Kondoh K, Lu Z, Ye X, Olson DP, Lowell BB, Buck LB (2016) A specific area of olfactory cortex involved in stress hormone responses to predator odours. *Nature* 532:103–6.
- Kreitzer AC, Regehr WG (2001) Retrograde inhibition of presynaptic calcium influx by endogenous cannabinoids at excitatory synapses onto Purkinje cells. *Neuron* 29:717–27.
- Krentz AJ, Fujioka K, Hompesch M (2016) Evolution of pharmacological obesity treatments: focus on adverse side-effect profiles. *Diabetes, Obesity and Metabolism* 18:558–570.
- Krishnan V, Nestler EJ (2008) The molecular neurobiology of depression. *Nature* 455:894–902.
- Lépine JP, Briley M (2011) The increasing burden of depression. *Neuropsychiatr Dis Treat* 7:3–7.
- Lewis CM, Lazar AE (2013) Orienting towards ensembles: From single cells to neural populations. *J Neurosci* 33:2–3.
- Llorente-Berzal A, Terzian AL, di Marzo V, Micale V, Viveros MP, Wotjak CT (2015) 2-AG promotes the expression of conditioned fear via cannabinoid receptor type 1 on GABAergic neurons. *Psychopharmacology (Berl)* 232:2811–25.
- Loew LM (1992) Voltage-sensitive dyes: Measurement of membrane potentials induced by DC and AC electric fields. *Bioelectromagnetics Suppl* 1:179–89.
- Logothetis NK (2008) What we can do and what we cannot do with fMRI. *Nature* 453:869–78.

- Lutz B, Marsicano G, Maldonado R, Hillard CJ (2015) The endocannabinoid system in guarding against fear, anxiety and stress. *Nat Rev Neurosci* 16:705–18.
- Maggio N, Segal M (2007) Striking variations in corticosteroid modulation of long-term potentiation along the septotemporal axis of the hippocampus. *J Neurosci* 27:5757–65.
- Mangieri RA, Piomelli D (2007) Enhancement of endocannabinoid signaling and the pharmacotherapy of depression. *Pharmacol Res* 56:360–6.
- Marks DM, Pae CU, Patkar AA (2008) Triple reuptake inhibitors: the next generation of antidepressants. *Curr Neuropharmacol* 6:338–43.
- Marsch R, Foeller E, Rammes G, Bunck M, Kossel M, Holsboer F, Zieglgansberger W, Landgraf R, Lutz B, Wotjak CT (2007) Reduced anxiety, conditioned fear, and hippocampal long-term potentiation in transient receptor potential vanilloid type 1 receptor-deficient mice. *J Neurosci* 27:832–9.
- Marsicano G, Goodenough S, Monory K, Hermann H, Eder M, Cannich A, Azad SC, Cascio MG, Gutierrez SO, van der Stelt M, Lopez-Rodriguez ML, Casanova E, Schutz G, Zieglgansberger W, Di Marzo V, Behl C, Lutz B (2003) CB1 cannabinoid receptors and on-demand defense against excitotoxicity. *Science* 302:84–8.
- Marsicano G, Lutz B (1999) Expression of the cannabinoid receptor CB1 in distinct neuronal subpopulations in the adult mouse forebrain. *Eur J Neurosci* 11:4213–25.
- Matsuda LA, Lolait SJ, Brownstein MJ, Young AC, Bonner TI (1990) Structure of a cannabinoid receptor and functional expression of the cloned cDNA. *Nature* 346:561–4.
- Mechoulam R, Ben-Shabat S, Hanus L, Ligumsky M, Kaminski NE, Schatz AR, Gopher A, Almog S, Martin BR, Compton DR, et al. (1995) Identification of an endogenous 2-monoglyceride, present in canine gut, that binds to cannabinoid receptors. *Biochem Pharmacol* 50:83–90.
- Mechoulam R, Hanus LO, Pertwee R, Howlett AC (2014) Early phytocannabinoid chemistry to endocannabinoids and beyond. *Nat Rev Neurosci* 15:757–64.
- Micale V, Di Marzo V, Sulcova A, Wotjak CT, Drago F (2013) Endocannabinoid system and mood disorders: priming a target for new therapies. *Pharmacol Ther* 138:18–37.
- Micale V, Stepan J, Jurik A, Pamplona FA, Marsch R, Drago F, Eder M, Wotjak CT (2017) Extinction of avoidance behavior by safety learning depends on endocannabinoid signaling in the hippocampus. *Journal of Psychiatric Research* 90:46–59.
- Miller EW, Lin JY, Frady EP, Steinbach PA, Kristan WB J, Tsien RY (2012) Optically monitoring voltage in neurons by photo-induced electron transfer through molecular wires. *Proc Natl Acad Sci U S A* 109:2114–9.
- Mizuseki K, Sirota A, Pastalkova E, Buzsáki G (2009) Theta oscillations provide temporal windows for local circuit computation in the entorhinal-hippocampal loop. *Neuron* 64:267–80.

- Monory K, Blaudzun H, Massa F, Kaiser N, Lemberger T, Schutz G, Wotjak CT, Lutz B, Marsicano G (2007) Genetic dissection of behavioural and autonomic effects of Delta(9)-tetrahydrocannabinol in mice. *PLoS Biol* 5:e269.
- Moreira FA, Aguiar DC, Terzian AL, Guimaraes FS, Wotjak CT (2012) Cannabinoid type 1 receptors and transient receptor potential vanilloid type 1 channels in fear and anxiety—two sides of one coin? *Neuroscience* 204:186–92.
- Morena M, Patel S, Bains JS, Hill MN (2016) Neurobiological Interactions Between Stress and the Endocannabinoid System. *Neuropsychopharmacology* 41:80–102.
- Mori K, Togashi H, Kojima T, Matsumoto M, Ohashi S, Ueno K, Yoshioka M (2001) Different effects of anxiolytic agents, diazepam and 5-HT(1A) agonist tandospirone, on hippocampal long-term potentiation in vivo. *Pharmacol Biochem Behav* 69:367–72.
- Munro S, Thomas KL, Abu-Shaar M (1993) Molecular characterization of a peripheral receptor for cannabinoids. *Nature* 365:61–5.
- Nakashiba T, Young JZ, McHugh TJ, Buhl DL, Tonegawa S (2008) Transgenic inhibition of synaptic transmission reveals role of CA3 output in hippocampal learning. *Science* 319:1260–1264.
- Neher E, Sakmann B (1976) Single-channel currents recorded from membrane of denervated frog muscle fibres. *Nature* 260:799–802.
- Neves G, Cooke SF, Bliss TV (2008) Synaptic plasticity, memory and the hippocampus: A neural network approach to causality. *Nat Rev Neurosci* 9:65–75.
- Nicoll RA, Schmitz D (2005) Synaptic plasticity at hippocampal mossy fibre synapses. *Nat Rev Neurosci* 6:863–76.
- Ohno-Shosaku T, Kano M (2014) Endocannabinoid-mediated retrograde modulation of synaptic transmission. *Curr Opin Neurobiol* 29:1–8.
- Ohno-Shosaku T, Maejima T, Kano M (2001) Endogenous cannabinoids mediate retrograde signals from depolarized postsynaptic neurons to presynaptic terminals. *Neuron* 29:729–38.
- Otmakhova NA, Lisman JE (1996) D1/D5 dopamine receptor activation increases the magnitude of early long-term potentiation at CA1 hippocampal synapses. *J Neurosci* 16:7478–86.
- Patton PE, McNaughton B (1995) Connection matrix of the hippocampal formation: I. The dentate gyrus. *Hippocampus* 5:245–86.
- Pertwee RG (2015) Endocannabinoids and Their Pharmacological Actions. *Handb Exp Pharmacol* 231:1–37.
- Péterfi Z, Urbán GM, Papp OI, Németh B, Monyer H, Szabó G, Erdélyi F, Mackie K, Freund TF, Hájos N, Kátona I (2012) Endocannabinoid-mediated long-term depression of afferent excitatory synapses in hippocampal pyramidal cells and GABAergic interneurons. *J Neurosci* 32:14448–63.
- Peterka DS, Takahashi H, Yuste R (2011) Imaging voltage in neurons. *Neuron* 69:9–21.

- Quilichini P, Sirota A, Buzsáki G (2010) Intrinsic circuit organization and theta-gamma oscillation dynamics in the entorhinal cortex of the rat. *J Neurosci* 30:11128–42.
- Radley JJ (2012) Toward a limbic cortical inhibitory network: Implications for hypothalamic-pituitary-adrenal responses following chronic stress. *Front Behav Neurosci* 6:7.
- Rammes G, Rupprecht R (2007) Modulation of ligand-gated ion channels by antidepressants and antipsychotics. *Mol Neurobiol* 35:160–74.
- Ravindran LN, Stein MB (2010) The pharmacologic treatment of anxiety disorders: a review of progress. *J Clin Psychiatry* 71:839–54.
- Reardon S (2016) Mysterious antidepressant target reveals its shape. *Nature News*, Apr 6, 2016 .
- Refojo D, Schweizer M, Kuehne C, Ehrenberg S, Thoeringer C, Vogl AM, Dedic N, Schumacher M, von Wolff G, Avrabos C, Touma C, Engblom D, Schütz G, Nave KA, Eder M, Wotjak CT, Sillaber I, Holsboer F, Wurst W, Deussing JM (2011) Glutamatergic and dopaminergic neurons mediate anxiogenic and anxiolytic effects of CRHR1. *Science* 333:1903–7.
- Ressler KJ, Mayberg HS (2007) Targeting abnormal neural circuits in mood and anxiety disorders: From the laboratory to the clinic. *Nat Neurosci* 10:1116–24.
- Riebe CJ, Pamplona F, Kamprath K, Wotjak CT (2012) Fear relief-toward a new conceptual frame work and what endocannabinoids gotta do with it. *Neuroscience* 204:159–85.
- Rubino T, Zamberletti E, Parolaro D (2015) Endocannabinoids and Mental Disorders. *Handb Exp Pharmacol* 231:261–83.
- Rudolph U, Knoflach F (2011) Beyond classical benzodiazepines: novel therapeutic potential of GABAA receptor subtypes. *Nat Rev Drug Discov* 10:685–97.
- Rutishauser U, Ross IB, Mamelak AN, Schuman EM (2010) Human memory strength is predicted by theta-frequency phase-locking of single neurons. *Nature* 464:903–7.
- Sapolsky RM, Krey LC, McEwen BS (1986) The neuroendocrinology of stress and aging: The glucocorticoid cascade hypothesis. *Endocr Rev* 7:284–301.
- Sarinana J, Tonegawa S (2016) Differentiation of forebrain and hippocampal dopamine 1-class receptors, D1R and D5R, in spatial learning and memory. *Hippocampus* 26:76–86.
- Shimizu K, Matsubara K, Uezono T, Kimura K, Shiono H (1998) Reduced dorsal hippocampal glutamate release significantly correlates with the spatial memory deficits produced by benzodiazepines and ethanol. *Neuroscience* 83:701–6.
- Singewald N, Schmuckermair C, Whittle N, Holmes A, Ressler KJ (2015) Pharmacology of cognitive enhancers for exposure-based therapy of fear, anxiety and trauma-related disorders. *Pharmacol Ther* 149:150–90.
- Steel Z, Marnane C, Iranpour C, Chey T, Jackson JW, Patel V, Silove D (2014) The global prevalence of common mental disorders: a systematic review and meta-analysis 1980-2013. *Int J Epidemiol* 43:476–93.

- Stella N, Schweitzer P, Piomelli D (1997) A second endogenous cannabinoid that modulates long-term potentiation. *Nature* 388:773–8.
- Stempel AV, Stumpf A, Zhang HY, Ozdogan T, Pannasch U, Theis AK, Otte DM, Wojtalla A, Racz I, Ponomarenko A, Xi ZX, Zimmer A, Schmitz D (2016) Cannabinoid Type 2 Receptors Mediate a Cell Type-Specific Plasticity in the Hippocampus. *Neuron* .
- Stepan J (2015) Real-time imaging of hippocampal network dynamics reveals trisynaptic induction of CA1 LTP and "circuit-level" effects of chronic stress and antidepressants. *PhD Thesis*. Ludwig Maximilians University Munich.
- Stepan J, Dine J, Eder M (2015a) Functional optical probing of the hippocampal trisynaptic circuit in vitro: network dynamics, filter properties, and polysynaptic induction of CA1 LTP. *Front Neurosci* 9:160.
- Stepan J, Dine J, Fenzl T, Polta SA, von Wolff G, Wotjak CT, Eder M (2012) Entorhinal theta-frequency input to the dentate gyrus trisynaptically evokes hippocampal CA1 LTP. *Front Neural Circuits* 6:64.
- Stepan J, Hladky F, Uribe A, Holsboer F, Schmidt MV, Eder M (2015b) High-Speed imaging reveals opposing effects of chronic stress and antidepressants on neuronal activity propagation through the hippocampal trisynaptic circuit. *Front Neural Circuits* 9:70.
- Strange BA, Witter MP, Lein ES, Moser EI (2014) Functional organization of the hippocampal longitudinal axis. *Nat Rev Neurosci* 15:655–69.
- Sugiura T, Kondo S, Sukagawa A, Nakane S, Shinoda A, Itoh K, Yamashita A, Waku K (1995) 2-Arachidonoylglycerol: a possible endogenous cannabinoid receptor ligand in brain. *Biochem Biophys Res Commun* 215:89–97.
- Terranova JP, Michaud JC, Le Fur G, Soubrie P (1995) Inhibition of long-term potentiation in rat hippocampal slices by anandamide and WIN55212-2: reversal by SR141716 A, a selective antagonist of CB1 cannabinoid receptors. *Naunyn Schmiedebergs Arch Pharmacol* 352:576–9.
- Teyler TJ, Rudy JW (2007) The hippocampal indexing theory and episodic memory: updating the index. *Hippocampus* 17:1158–69.
- Timic T, Joksimovic S, Milic M, Divljakovic J, Batinic B, Savic MM (2013) Midazolam impairs acquisition and retrieval, but not consolidation of reference memory in the Morris water maze. *Behav Brain Res* 241:198–205.
- Tokuda K, O'Dell KA, Izumi Y, Zorumski CF (2010) Midazolam inhibits hippocampal long-term potentiation and learning through dual central and peripheral benzodiazepine receptor activation and neurosteroidogenesis. *J Neurosci* 30:16788–95.
- Tominaga T, Tominaga Y, Yamada H, Matsumoto G, Ichikawa M (2000) Quantification of optical signals with electrophysiological signals in neural activities of Di-4-ANEPPS stained rat hippocampal slices. *J Neurosci Methods* 102:11–23.
- van Strien NM, Cappaert NL, Witter MP (2009) The anatomy of memory: An interactive overview of the parahippocampal-hippocampal network. *Nat Rev Neurosci* 10:272–82.

- von Wolff G, Avrabos C, Stepan J, Wurst W, Deussing JM, Holsboer F, Eder M (2011) Voltage-sensitive dye imaging demonstrates an enhancing effect of corticotropin-releasing hormone on neuronal activity propagation through the hippocampal formation. *Journal of Psychiatric Research* 45:256–261.
- Watanabe Y, Gould E, McEwen BS (1992) Stress induces atrophy of apical dendrites of hippocampal CA3 pyramidal neurons. *Brain Res* 588:341–5.
- Watson C, Paxinos G, Puelles L (2011) *The Mouse Nervous System* Elsevier Science.
- Whitlock JR, Heynen AJ, Shuler MG, Bear MF (2006) Learning induces long-term potentiation in the hippocampus. *Science* 313:1093–7.
- WHO (2004) *The global burden of disease: 2004 update*. Geneva, Switzerland: World Health Organization.
- Wilson RI, Nicoll RA (2001) Endogenous cannabinoids mediate retrograde signalling at hippocampal synapses. *Nature* 410:588–92.
- Wiskerke J, Irimia C, Cravatt BF, De Vries TJ, Schoffelmeer AN, Pattij T, Parsons LH (2012) Characterization of the effects of reuptake and hydrolysis inhibition on interstitial endocannabinoid levels in the brain: an in vivo microdialysis study. *ACS Chem Neurosci* 3:407–17.
- Witter MP (2007) The perforant path: Projections from the entorhinal cortex to the dentate gyrus. *Prog Brain Res* 163:43–61.
- Witter MP, Wouterlood FG, Naber PA, Van Haften T (2000) Anatomical organization of the parahippocampal-hippocampal network. *Ann N Y Acad Sci* 911:1–24.
- Wrobel S (2007) Science, serotonin, and sadness: The biology of antidepressants: A series for the public. *FASEB J* 21:3404–17.
- Yizhar O, Fenno LE, Prigge M, Schneider F, Davidson TJ, O’Shea DJ, Sohal VS, Goshen I, Finkelstein J, Paz JT, Stehfest K, Fudim R, Ramakrishnan C, Huguenard JR, Hegemann P, Deisseroth K (2011) Neocortical excitation/inhibition balance in information processing and social dysfunction. *Nature* 477:171–8.
- Zanos P, Moaddel R, Morris PJ, Georgiou P, Fischell J, Elmer GI, Alkondon M, Yuan P, Pribut HJ, Singh NS, Dossou KS, Fang Y, Huang XP, Mayo CL, Wainer IW, Albuquerque EX, Thompson SM, Thomas CJ, Zarate CA J, Gould TD (2016) NMDAR inhibition-independent antidepressant actions of ketamine metabolites. *Nature* 533:481–6.
- Zemelman BV, Lee GA, Ng M, Miesenbock G (2002) Selective photostimulation of genetically chARGed neurons. *Neuron* 33:15–22.
- Zhang F, Gradinaru V, Adamantidis AR, Durand R, Airan RD, de Lecea L, Deisseroth K (2010) Optogenetic interrogation of neural circuits: technology for probing mammalian brain structures. *Nature Protocols* 5:439–56.
- Zygmunt PM, Chuang H, Movahed P, Julius D, Hogestatt ED (2000) The anandamide transport inhibitor AM404 activates vanilloid receptors. *Eur J Pharmacol* 396:39–42.

Chapter 7

Appendix

7.1 Chemicals

Tab. 7.1. Chemicals

SUBSTANCE	CHEMICAL NAME	SUPPLIER/CAT.NR.	SOLVING MEDIUM
ACSF SALTS	-	Sigma Aldrich/-	Aqua dest.
AM404	N-(4-Hydroxyphenyl)-5Z,8Z,11Z,14Z-eicosatetraenamide	Tocris/1116	DMSO
1(S),9(R)-(-)-BICUCULLINE METHIODIDE	[R-(R*,S*)]-5-(6,8-Dihydro-8-oxofuro[3,4-e]-1,3-benzodioxol-6-yl)-5,6,7,8-tetrahydro-6,6-dimethyl-1,3-dioxolo[4,5-g]isoquinolinium iodide	Sigma-Aldrich/14343	ACSF
DMSO	Dimethyl sulfoxide	Sigma-Aldrich/PHR1309	-
DI-4-ANEPPS	4-(2-(6-(Dibutylamino)-2-naphthalenyl)ethenyl)-1-(3-sulfopropyl)pyridinium hydroxide inner salt	Sigma-Aldrich/D8064	DMSO
DIAZEPAM	7-Chloro-1-methyl-5-phenyl-3H-1,4-benzodiazepin-2(1H)-one	Sigma-Aldrich/D0899	DMSO
ISOFLURANE	(±)-Difluoromethoxy-1-chlor-2,2,2-trifluorethan	Abbott/B506	-

(Abbott, Illinois, USA; Sigma-Aldrich, St. Louis, USA; Tocris, Bristol, UK)